

A ^{125}Te AND ^{129}I MOSSBAUER STUDY OF
THE COMPOUNDS TeX_4 AND $(\text{NH}_4)_2\text{TeX}_6$
WHERE X = Cl, Br, I.

by

Joyce Janet Johnstone

B.Sc., Simon Fraser University, 1969.

A THESIS SUBMITTED IN PARTIAL
FULFILLMENT OF THE REQUIREMENTS
FOR THE DEGREE OF
MASTER OF SCIENCE
in the Department
of
Chemistry

C JOYCE JANET JOHNSTONE 1972

SIMON FRASER UNIVERSITY

July 1972

APPROVAL

Name: Joyce Janet Johnstone
Degree: Master of Science
Title of Thesis: A ^{125}Te and ^{129}I Mössbauer Study of
the Compounds TeX_4 and $(\text{NH}_4)_2\text{TeX}_6$
Where X = Cl, Br, I.

Examining Committee:

C.H.W. Jones
Senior Supervisor

I.D. Gay

D.G. Tuck

E.J. Wells

Date Approved: 5^o September 1972

ABSTRACT

The ^{129}I Mössbauer emission spectra of the compounds $(\text{NH}_4)_2^{129\text{m}}\text{TeX}_6$ and $^{129\text{m}}\text{TeX}_4$ ($X = \text{Cl}, \text{Br}, \text{I}$) have been reported against a Na^{129}I absorber at 4°K . The spectra give evidence in the case of the $(\text{NH}_4)_2\text{TeX}_6$ compounds for the formation in the radioactive decay of the octahedral ions ICl_6^- , IBr_6^- and II_6^- , which are observed over the lifetime of the Mössbauer transition. It is shown that the ^{129}I isomer shifts for these ions are consistent with the values to be expected from the ^{125}Te isomer shifts of the parent compounds, and the previously reported $^{125}\text{Te}/^{129}\text{I}$ isomer shift ratio.

In the TeX_4 compounds, the emission spectra are much more complex and indicate that the ^{129}I atoms are not found in an environment isostructural and isoelectronic with that of the parent. These spectra are tentatively interpreted as evidence for the presence of the square planar IX_4^- ions in each case.

The ^{125}Te Mössbauer absorption spectra of the parent compounds were also studied to aid in their identification, and the parameters obtained are compared with those in the literature. The ^{125}Te isomer shifts for the TeX_6^{2-} anions are interpreted in terms of pure p-bonding

and, in conjunction with data from the emission spectra and data from previously reported N.Q.R. work, an isomer shift versus p-hole density relationship is established for tellurium:

$$\delta(\text{mm. sec.}^{-1}) = 0.45(\pm 0.01)h_p - 0.15(\pm 0.03)$$

(I/Cu sources)

It is shown that this expression is consistent with that previously derived by other workers for ^{129}I Mössbauer isomer shifts.

TABLE OF CONTENTS

CHAPTER	PAGE
I.	Introduction 1
II.	Mössbauer Studies of the Effects of Radioactive Decay 3
A.	Mössbauer Studies of Beta Decay 3
1.	No Molecular Fragmentation 3
2.	Molecular Fragmentation 4
B.	Mössbauer Studies of Electron Capture and Isomeric Transition 5
III.	The Mössbauer Effect 6
A.	Isomer Shift 6
B.	Quadrupole Coupling 7
IV.	^{125}Te Mössbauer 10
A.	Isomer Shift 11
B.	Quadrupole Coupling 14
V.	^{129}I Mössbauer 15
A.	Isomer Shift 15
B.	Quadrupole Coupling 20
VI.	^{127}I Mössbauer 23
VII.	Nuclear Quadrupole Resonance Spectroscopy . 25
A.	N.Q.R. of Tellurium Compounds 26
B.	N.Q.R. Studies on Polyhalogens 27

VIII.	The Structure and Properties of the Tellurium Halides and the Polyhalogen Compounds	29
A.	Tellurium Halides	29
	1. Hexahalides	29
	2. Tetrahalides	31
B.	Polyhalogens	33
IX.	Experimental	38
A.	The Mössbauer Spectrometer	38
B.	Preparation of the Compounds	40
	1. TeX_4 , X = Cl, Br, I	40
	2. TeI_4	40
	3. $(\text{NH}_4)_2\text{TeX}_6$	41
	4. ZnTe	41
C.	Raman Spectra	41
D.	Mössbauer Experiments with ^{125}Te	43
	1. $^{125}\text{I}/\text{Cu}$ Source	44
	2. ^{125}Te Absorber Compounds	44
E.	Mössbauer Experiments with ^{129}I	44
	1. Source Activities for ^{129}I Emission Experiments	45
	2. Absorber	46
F.	Computer Analysis of Mössbauer Spectra	46

Y.	Results	48
A.	^{125}Te Absorption Spectra	48
B.	^{129}I Emission Spectra	51
	1. Emission Spectra of the $(\text{NH}_4)_2^{129\text{m}}\text{TeX}_6$ Compounds	52
	2. Emission Spectra of the $^{129\text{m}}\text{TeX}_4$ Compounds	59
	3. The Emission Spectrum of $^{129}\text{TeCl}_4$	62
	4. The Absorption Spectrum of $\text{Te}^{129}\text{I}_4$	64
XI.	Discussion of the ^{125}Te Mössbauer Absorption Spectra	65
A.	Significance of TeX_6^{2-} Isomer Shifts	65
B.	Significance of the TeX_4 Isomer Shifts and Quadrupole Couplings	67
	1. Isomer Shift	67
	2. Quadrupole Coupling	68
XII.	Discussion of the ^{129}I Mössbauer Spectra	69
A.	Identification of the IX_6^- Anions	69
B.	Significance of observing IX_6^- Anions	73
C.	Electron Recall Following β -Decay	75
D.	^{125}Te Isomer Shift Relationships	76
E.	Possibility of d-Orbital Participation in Bonding	79
F.	The Decay Products of $^{129\text{m}}\text{TeX}_4$	81
XIII.	Conclusion	88
XIV	List of References	93

LIST OF TABLES

TABLE		PAGE
I.	Atomic Quadrupole Coupling Constants eqQ Atom of Halogens	25
II.	Crystal Structures of the Tellurium Halides	29
III.	A. The Polyhalide ions	34
	B. The Interhalogens	34
IV.	Raman Spectra of the Tellurium Halides	42
V.	Elemental Analysis Results for Tellurium and Halogen Content	43
VI.	^{125}Te Mössbauer Absorption Parameters	50
VII.	$(\text{NH}_4)_2\text{TeX}_6$ Mössbauer Emission Experimental Data	53
VIII.	A. TeX_4 Mössbauer Emission Parameters	61
	B. $\text{Te}^{129}\text{I}_4$ Mössbauer Absorption Parameters	61
IX.	The Tellurium 5p Shell Electron Populations and the ^{125}Te Mössbauer Isomer Shifts of the TeX_6^{2-} Ions (X = Cl, Br, I)	66
X.	Comparison of Mössbauer and N.Q.R. Results	72
XI.	Predicted ^{129}I δ and e^2qQ from ^{125}Te Data	82
XII.	A Comparison of the Predicted Line Positions for $^{129}\text{ICl}_4^+$ Mössbauer Emission to the Experimentally Observed Positions	83
XIII.	A. Table of Orbital Populations U _l and h _p Values for the ^{129m}Te Mössbauer Emission Data in the Decay $^{129m}\text{TeX}_4 \xrightarrow{\beta^-} ^{129}\text{IX}_4^+$	85
	B. Comparison of $^{129m}\text{TeCl}_4$ Emission and $^{127}\text{ICl}_4^-$ Absorption Mössbauer Spectra.	85

LIST OF FIGURES

FIGURE		PAGE
1.	Decay Scheme Showing the Population of the Mössbauer Transition in ^{125}Te	10
2.	A Comparison of Isomer Shifts for ^{125}Te -Labelled Tellurium Compounds	13
3.	Decay Scheme Showing the Population of the Mössbauer Transition in ^{129}I	16
4.	^{129}I Quadrupole Splitting for e^2qQ_{I}/h	17
5.	A Comparison of Isomer Shifts for ^{129}I Labelled Iodine Compounds	19
6.	Decay Scheme Showing the Population of the Mössbauer Transition in ^{127}I	24
7.	Orbital Populations in ICl_4^- and ICl_2^-	28
8.	Crystal Structure of TeCl_4	30
9.	Diagram of the Mössbauer Spectrometer	39
10.	^{125}Te Absorption Spectra of the TeX_4 (X = Cl, Br, I) Compounds	49
11.	^{129}I Mössbauer Emission Spectra of $(\text{NH}_4)_2\text{TeBr}_6$	54
12.	^{129}I Emission Spectra of the $(\text{NH}_4)_2\text{TeX}_6$ (X = Cl, Br, I) Compounds	55
13.	^{129}I Emission Spectrum of $(\text{NH}_4)_2\text{TeI}_6$	56
14.	^{129}I Emission Spectra of the TeX_4 (X = Cl, Br, I) Compounds	60
15.	^{129}I Emission Spectrum of TeCl_4	63

16.	Isomer Shift Plot of $\delta(^{125}\text{Te})$ Versus $\delta(^{129}\text{I})$ for Isoelectronic and Isostructural Compounds	70
17.	Comparison of $\delta(^{125}\text{Te})$ Versus $h\nu$ From N.Q.R. Data Assuming (a) 15% and (b) No s-Character in the Halogen Bonding Orbitals	78

ACKNOWLEDGMENT

The author would like to express her gratitude to her Research Supervisor, Dr. C.H.W. Jones, for his advice and guidance throughout this work.

Sincere thanks are also extended to:

The National Research Council for financial support in the form of a post-graduate scholarship;

Dr. F. Brown at Atomic Energy of Canada Limited, for his assistance in performing the reactor irradiations involved in this work.

Dr. P. Vasudev for writing and revising programs used in this work;

The occupants of the Nuclear Suite at Simon Fraser University for their assistance in many ways;

and finally to my parents, Mr. and Mrs. W.M. Johnstone, for their continued support throughout my academic career.

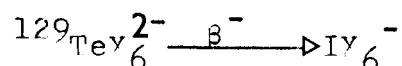
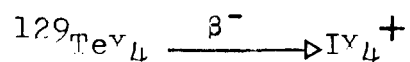
I. Introduction.

Radioactive decay may be used as a tool to prepare and study chemical compounds, which have not previously been prepared by more conventional techniques. The objective of this work was to study the formation of several novel, polyhalogen complex ions in the solid state following radioactive decay and to study the bonding in these compounds using the Mössbauer effect. The radioactive decay event serves both to synthesize the new molecule and to populate the Mössbauer level in the daughter nuclide. The Mössbauer isomer shift and quadrupole coupling data obtained may then be related to the electronic structure of the newly formed molecule, nanoseconds after it has been formed in the crystal.

In such an experiment the interpretation of the Mössbauer spectra obtained is greatly simplified if the nature of the bonding in the parent molecule has been previously studied by Mössbauer and nuclear quadrupole resonance spectroscopy, and if the structure has been determined by X-ray crystallography. Such studies have previously been carried out for the parent tellurium compounds used in the present work and the relevant information obtained will be reviewed in later sections. In addition, previous studies of the bonding and structures of the interhalogen compounds using Mössbauer and N.Q.R. techniques are of obvious interest in the present context and will also be

reviewed.

The objective of the present investigation was to study the molecules formed in the radioactive decay of $^{129}\text{Te} \xrightarrow{\beta^-} ^{129}\text{I}$ in ^{129}Te labelled TeY_4 and TeY_6^{2-} compounds, where $Y = \text{Cl}, \text{Br}, \text{or I}$. When the radioactive decay is not accompanied by molecular fragmentation, the iso-electronic and isostructural iodine analogue of the parent tellurium molecule will be formed as shown below.



It was of interest to determine whether these unusual and novel iodine compounds would **exist as stable** chemical species over the lifetime of the Mössbauer transition.

II. Mössbauer Studies of the Effects of Radioactive Decay [1,2,3].

In radioactive decay, the nuclear transformation is often accompanied by fragmentation of the parent molecule as a consequence of electronic excitation resulting from the nuclear process.

In beta decay, the electron cloud of the atom is not disturbed, i.e. there is little or no excitation. By contrast in an isomeric transition which is highly internally converted or in electron capture, a hole is created in the inner shell of the decaying atom, leading to extensive ionization through Auger charging. As a result, beta decay rarely results in bond rupture, whereas internal conversion and electron capture usually lead to extensive molecular decomposition, at least in the gas phase.

A. Mössbauer Studies of Beta Decay.

1. No Molecular Fragmentation.

G.J. Perlow and M.R. Perlow [4] first used the Mössbauer effect to study daughter molecules synthesized in beta decay. In the initial work of Perlow and Perlow the ^{127}I emission spectrum of $\text{H}_6^{127\text{m}}\text{TeO}_6$ was studied. Here the decay of $^{127\text{m}}\text{Te}$ proceeds directly to the 57.6 keV. Mössbauer transition in ^{127}I by beta decay and it was concluded that the beta decay did not result in observable molecular disruption. Pasternak [5] repeated the above

experiment, only now using the ^{129}I Mössbauer transition as a probe. Again the isomer shift of the ^{129}I spectrum corresponded to that of IO_6^{5-} .

Perlow and Perlow^[6] also investigated the formation of the xenon compounds XeCl_4 and XeCl_2 from the beta decay of ICl_2^- and ICl_4^- labelled with ^{129}I . The xenon compounds were found to be stable over the one nanosecond lifetime of the 39.58 keV, isomeric level in ^{129}Xe .

Work done in this laboratory by Jones and Warren^[7] utilized the beta decay of $^{129}\text{Te} \xrightarrow{\beta^-} ^{129}\text{I}$ in various tellurium oxygen compounds to populate the 27.7 keV, Mössbauer level in iodine. They found no molecular fragmentation in the product iodine compounds. It was also shown that the ICl_6^- ion formed in the decay $^{129}\text{TeCl}_6^{2-} \xrightarrow{\beta^-} ^{129}\text{ICl}_6^-$ remained stable. This discovery laid the basis for the present research.

2. Molecular Fragmentation.

Rother, Wagner and Zahn^[8] studied the chemical consequences of the beta decay of ^{193}Ir in several osmium compounds using the 73 keV., 6 nanosecond Mössbauer transition in ^{193}Ir . They observed that the primary daughter molecule formed in the beta decay $^{193}\text{Os} \xrightarrow{\beta^-} ^{193}\text{Ir}$ was not stable. This experiment is one of the very few cases in which molecular decomposition has been observed in simple beta decay.

Pasternak and Sonnino [9] used the 9.3 keV., 147 nanosecond Mössbauer level in ^{83}Kr to study the effects of the beta decay $^{83}\text{Br} \longrightarrow ^{83}\text{Kr}$ in various bromine compounds. For example, they found that in experiments with $^{83}\text{BrO}_3^-$ the corresponding $^{83}\text{KrO}_3$ species was not detected. In the case of the $^{129}\text{I} \xrightarrow{\beta^-} ^{129}\text{Xe}$ decay, discussed earlier, the formation of Xe compounds was probably observed because the ^{129}I beta decay populates the Mössbauer level of ^{129}Xe . In contrast in the ^{83}Br case the decay to the Mössbauer level occurs through the metastable state ($t_{1/2} = 1.9$ hr.) of ^{83}Kr . It is then possible that within this time the ^{83}Kr ion, formerly in a high-valence state, is transformed into a neutral atom.

B. Mössbauer Studies of Electron Capture and Isomeric Transition (EC and IT).

Violet and Booth [10], and subsequently Jung and Trifthäuser [11], investigated the effects of electron capture and Auger charging in the $^{125}\text{I} \xrightarrow{\text{EC}} ^{125}\text{Te}$ decay. In this investigation molecular fragmentation was observed in $\text{Na}^{125}\text{IO}_3$, as a result of the enormous excitation and ionization created in the Auger cascade accompanying the electron capture. Jones and Warren [7], in their studies on the decay $^{129\text{m}}\text{Te} \xrightarrow{\text{IT}} ^{129}\text{Te} \xrightarrow{\beta^-} ^{129}\text{I}$, also observed molecular fragmentation in a considerable fraction of the $^{129\text{m}}\text{Te} \longrightarrow ^{129}\text{Te}$ decay events in tellurium oxygen compounds.

III. The Mössbauer Effect.

The Mössbauer effect was discovered in 1958 by Rudolf Mössbauer^[12]. Applications of the effect have rapidly expanded to cover many aspects of physical and chemical phenomena.

Many books and articles have been written on the subject [13, 14, 15, 16] giving a complete description of its origin and uses in detail. A brief discussion of the Mössbauer parameters of importance in this research project is presented below.

A. Isomer Shift.

Only when both the source and absorber are subjected to the same physical conditions such as equal temperatures and equal local fields of their constituent nuclei will a Mössbauer spectrum be symmetric about zero velocity. Any deviation from zero velocity is an isomer shift which is directly related to the perturbation caused by the density of the s-electrons $|\psi_s(0)|^2$ at the source and absorber nuclei according to the expression:

$$\delta = \text{constant} \left[|\psi_s(0)|_a^2 - |\psi_s(0)|_s^2 \right] \left(\frac{\delta R}{R} \right) \quad (\text{III-1})$$

where $\delta R = R_{\text{ex}} - R_{\text{gnd}}^*$ and $R = \frac{R_{\text{ex}} + R_{\text{gnd}}}{2}$. The subscripts "a"

* ex - excited, gnd - ground

and "s" refer to absorbing and source nuclei respectively. The relationship between the sign of the observed isomer shift, the change in nuclear radius of the ground and excited states, and the change in s-electron density at the nucleus for any given Mössbauer source-absorber combination is shown below.

$\delta > 0$	$R_{ex} - R_{gnd} > 0$	$ \psi_s(0) _a > \psi_s(0) _s$	s	a	<u>e.g.</u>
	$R_{ex} - R_{gnd} < 0$	$ \psi_s(0) _a < \psi_s(0) _s$			$^{129}\text{I}, ^{125}\text{Te}$
					^{127}I
					$^{129}\text{I}, ^{126}\text{Te}$
					^{127}I

It is difficult to obtain information on s-electron densities from a single isomer shift, since both source and absorber s-electron densities are included. However, by measuring relative shifts for a series of compounds with respect to a standard source or absorber, the relative change in s-electron density can be determined.

B. Quadrupole Coupling e^2qQ .

Under the influence of an electric field gradient, the energy levels resulting from the quadrupole hyperfine splitting of a nuclear energy level are given by:

$$E_{m,I} = \frac{e^2 q Q}{4I(2I-1)} (C_0 - C_2 \eta^2) \quad (\text{III-2})$$

where

$$C_0 = 3m^2 - I(I+1) \quad (\text{III-3})$$

$$C_2 = \frac{1}{12} \left| \frac{f(I,m-1)}{m-1} - \frac{f(I,m+1)}{m+1} \right| \quad (\text{III-4})$$

$$f(I,m) = \frac{1}{4}(I^2 - m^2) [(I+1)^2 - m^2] \quad (\text{III-5})$$

assuming only terms up to η^2 need be considered. Here eQ is the electric field gradient in the z direction (the symmetry axis of the field) at the nuclear site, which has its origin in the distribution of electrons in the atom containing the Mössbauer nucleus. eQ is the nuclear quadrupole moment, I is the nuclear spin ($I \geq 1$) and m refers to the z component of the nuclear spin, I .

We define the deviation of the electric field gradient η in a molecule from axial symmetry by the equation:

$$\eta = \frac{V_{xx} - V_{yy}}{V_{zz}} \quad (\text{III-6})$$

(V_{jj} being the electric field gradient in direction j).

The interpretation of the quadrupole splitting of the ^{129}I Mössbauer spectrum requires one to take into account the splitting of the nuclear energy levels of the ground and the excited state. Hence the position of each line δ_{ij} corresponding to the $m_i - m_j$ transition in a quadrupole split spectrum is given by the expression^[17]

$$\delta_{ij} = \frac{ce^2qQ}{4E_\gamma} \left[\frac{Q^*}{Q} - \frac{(C_0^* - C_2^*\eta^2)}{I^*(2I-1)} - \frac{(C_0 - C_2\eta^2)}{I(2I-1)} \right] + \delta \quad (\text{III-7})$$

where δ is the isomer shift of the centroid of the Mössbauer spectrum with respect to zero velocity. The superscript ^{*} denotes the excited nuclear state, E_γ is the energy of the Mössbauer transition, and c is the velocity of light.

IV. ^{125}Te Mössbauer.

^{125}Te Mössbauer absorption experiments on TeX_4 and $(\text{NH}_4)_2\text{TeX}_6$ ($X = \text{Cl}, \text{Br}, \text{I}$) were carried out to characterise these compounds by comparison of the ^{125}Te Mössbauer parameters with those values previously reported in the literature.

The Mössbauer transition for ^{125}Te and the methods by which it may be populated are shown in Figure 1.

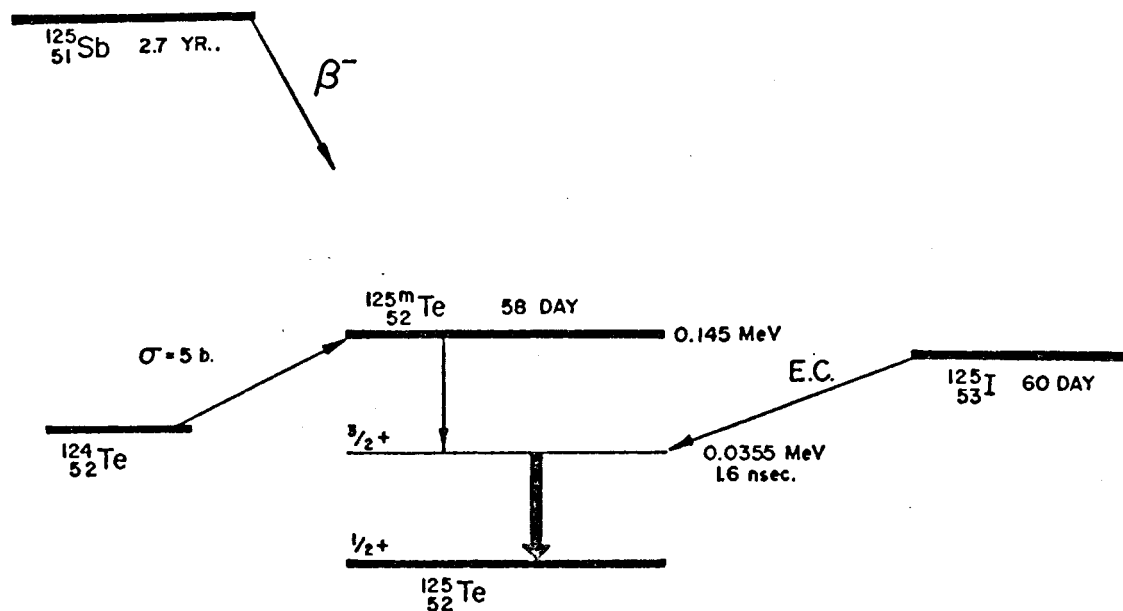


Figure 1. Decay Scheme Showing the Population of the Mössbauer Transition in ^{125}Te .

From preceding studies [10, 11, 18] it has been shown that the 35.5 keV., 1.6 nanosecond Mössbauer transition in ^{125}Te is characterised by a very large natural line width, $2\Gamma = 5.32 \text{ mm. sec.}^{-1}$ *, while the observed isomer shifts are relatively small as a consequence of a small $R_{ex}\text{-}R_{\text{end}}$ value. Moreover, the quadrupole coupling constants e^2qQ , observed for tellurium nuclei in an electrostatic field gradient, q , are relatively small because of the small value of the quadrupole moment Q . This leads to unresolved spectra and difficulties in spectra analysis. The line spacing Δ in the two line ^{125}Te quadrupole split spectrum is given by [13]

$$\Delta = E_{3/2} - E_{1/2} = \frac{e^2qQ}{2} \left(1 - \frac{\eta^2}{3}\right)^{\frac{1}{2}} \quad (\text{IV-1})$$

Since only two lines are present in a quadrupole split spectrum, a value for η can not be obtained. $\frac{\delta R}{R}$ for ^{125}Te was found to be $(1.3 \pm 0.9) \times 10^{-4}$ [19]. This should only be taken as a rough estimate since other calculations [11, 39] yield values that differ by an order of magnitude.

Interpretation of ^{125}Te Mössbauer Spectra

A. Isomer Shift.

The isomer shift is measured by determining the shift of the centroid of the Mössbauer spectrum with respect to zero velocity.

* $1 \text{ mm. sec.}^{-1} \approx 10^{-7} \text{ eV.}$

Representative values of ^{125}Te isomer shifts are shown in Figure 2^[20].

The positive value for $\text{Rex-R}_{\text{end}}$ for ^{125}Te indicates that if the s-electron density $|\psi_s(0)|^2$ at the absorbing nucleus is greater than at the source nucleus, then the isomer shift will be positive in sign. Conversely, a low s-electron density at the absorbing nucleus corresponds to a large negative isomer shift.

Large positive values for the isomer shifts may be readily understood in terms of the following model for bonding in these compounds. The $5s^2$ electrons of the tellurium may be considered to form a stereochemically inactive "lone pair". This was suggested by D.S. Urch^[21] who has considered the nature of the bonding in hexa-halogen complexes of non-transition metals. He proposed that if the ns orbital (a_{1g}) of the central atom plays little part in the bonding then an extra pair of electrons may be accommodated in the a_{1g} antibonding molecular orbital, a "lone pair", without distorting the octahedral symmetry. He also argues that electrons in such ns orbitals will decrease the "effective electronegativity" of the p-electrons, thus allowing them to play a greater part in bonding. Therefore, the loss of p-electrons in bonding would then lead to increased de-shielding of the $5s^2$ electron "lone pair" from the nucleus, with a commensurate increase in $|\psi_s(0)|_a^2$ which would be evidenced

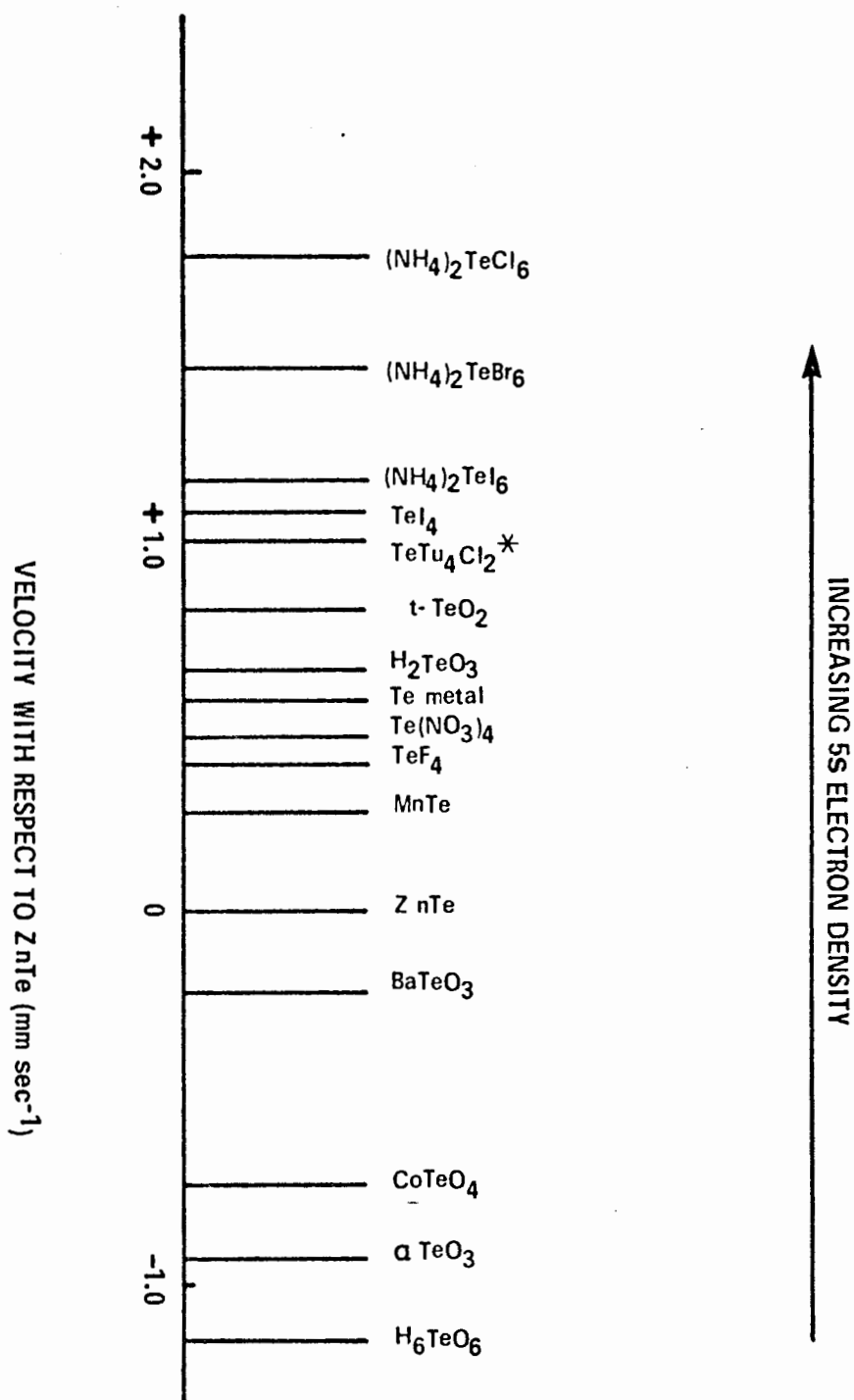


Figure 2. A Comparison of Isomer Shifts for ¹²⁵Te-Labelled Tellurium Compounds. A Positive Velocity Corresponds to the ZnTe Source Moving Towards the Absorber.

* Tu = (H₂N)₂CS

by an increasingly more positive isomer shift. For example if one compares the isomer shifts for the series TeX_6^{2-} ($X = \text{I, Br, Cl}$), they increase with the ligand going from I to Cl corresponding to an increase in the s-electron density at the tellurium nucleus. With the increase in electronegativity of the halogen more p-electron density from tellurium leads to a high s-electron density at the nucleus. Large negative isomer shifts may be explained by the presence of hybridization involving delocalization of the 5s electrons on the tellurium into bonding orbitals.

B. Quadrupole Coupling.

The parameter directly obtained from the ^{125}Te Mössbauer experiment is Δ the line spacing (Equation IV-1). When $\eta = 0$, that is the electric field gradient q is symmetrical about the z-axis, then:

$$\Delta = \frac{1}{2} e^2 q Q. \quad (\text{IV-2})$$

Hence, when $\eta \neq 0$ a value for $e^2 q Q$ can not be directly obtained, and therefore only comparisons of the Δ values can be made. Thus far very little useful information has been derived from ^{125}Te quadrupole splitting data in the literature. This may in part stem from the fact that many tellurium compounds are polymeric.

The nature of the ^{129}I Mössbauer transition has been well characterized and the decay scheme is shown in Figure 3. The 27.7 keV., 16.8 nanosecond ^{129}I Mössbauer transition yields a narrow natural line width, $2\Gamma = 0.59$ mm. sec.⁻¹ with relatively large isomer shifts and quadrupole coupling constants. However analysis of these Mössbauer spectra is complicated by the fact that the transition is a $5/2$ (excited)- $7/2$ (ground) transition and this leads to eight lines in the quadrupole split spectrum. In order to obtain the isomer shift, (Figure 4), the centroid of the eight line spectrum must be found using equation III-7. Cohen^[22] calculated the line positions for intervals of η and has shown that only the positions of lines four and eight are in fact sensitive to η . Therefore the parameters δ , e^2qQ and η can be determined from equation III-7 by:

1. using the positions of the lines other than four and eight to determine δ and e^2qQ ground by neglecting the terms in η^2 and
2. then determining η from the positions of lines four and eight.

Interpretation of ^{129}I Mössbauer Spectra.

A. Isomer Shift.

For ^{129}I Mössbauer spectra the relationship between the isomer shift and the s-electron density at the nucleus as given in equation III-1 becomes

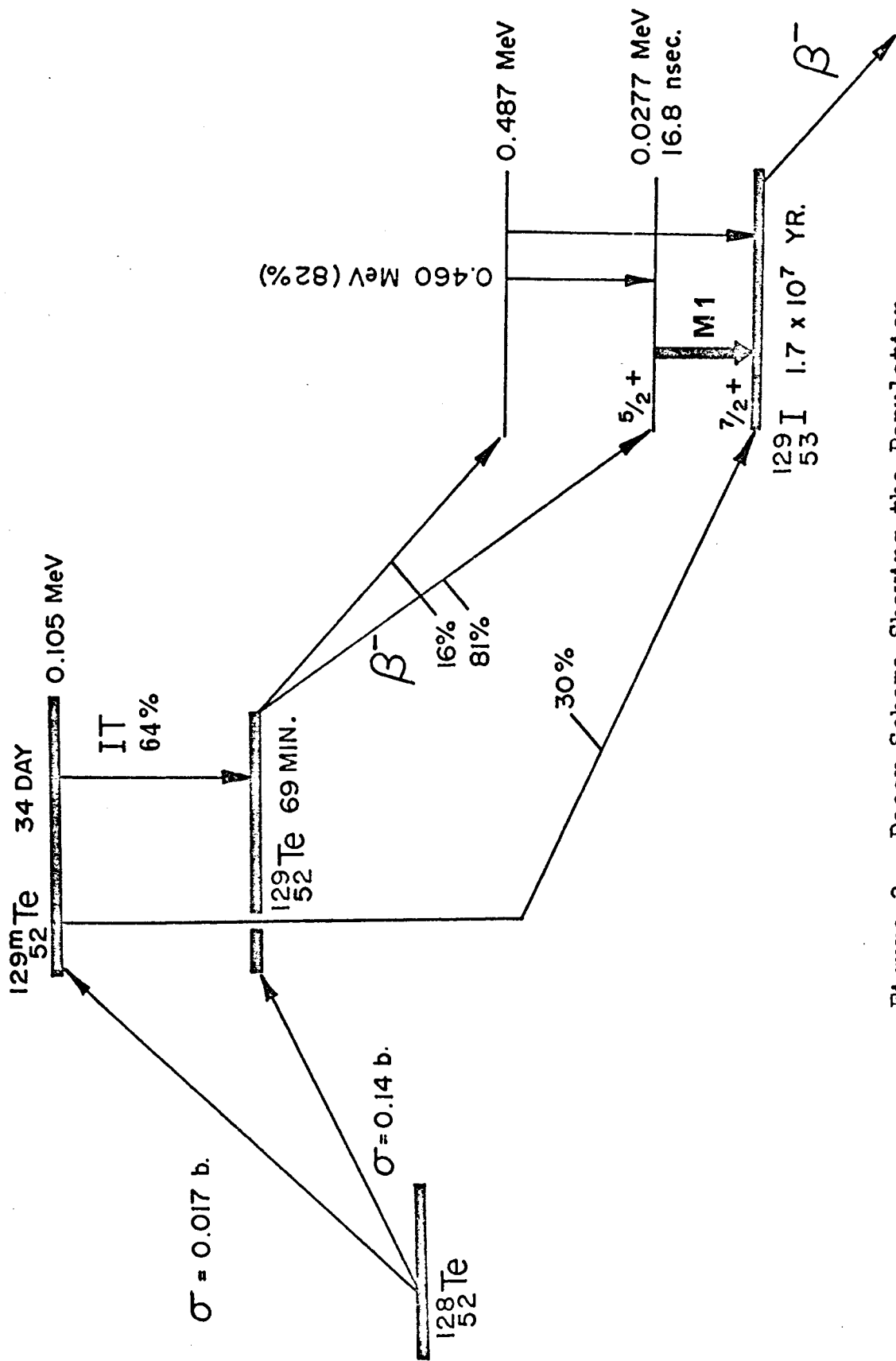


Figure 3. Decay Scheme Showing the Population of the Mössbauer Transition in ^{129}I .

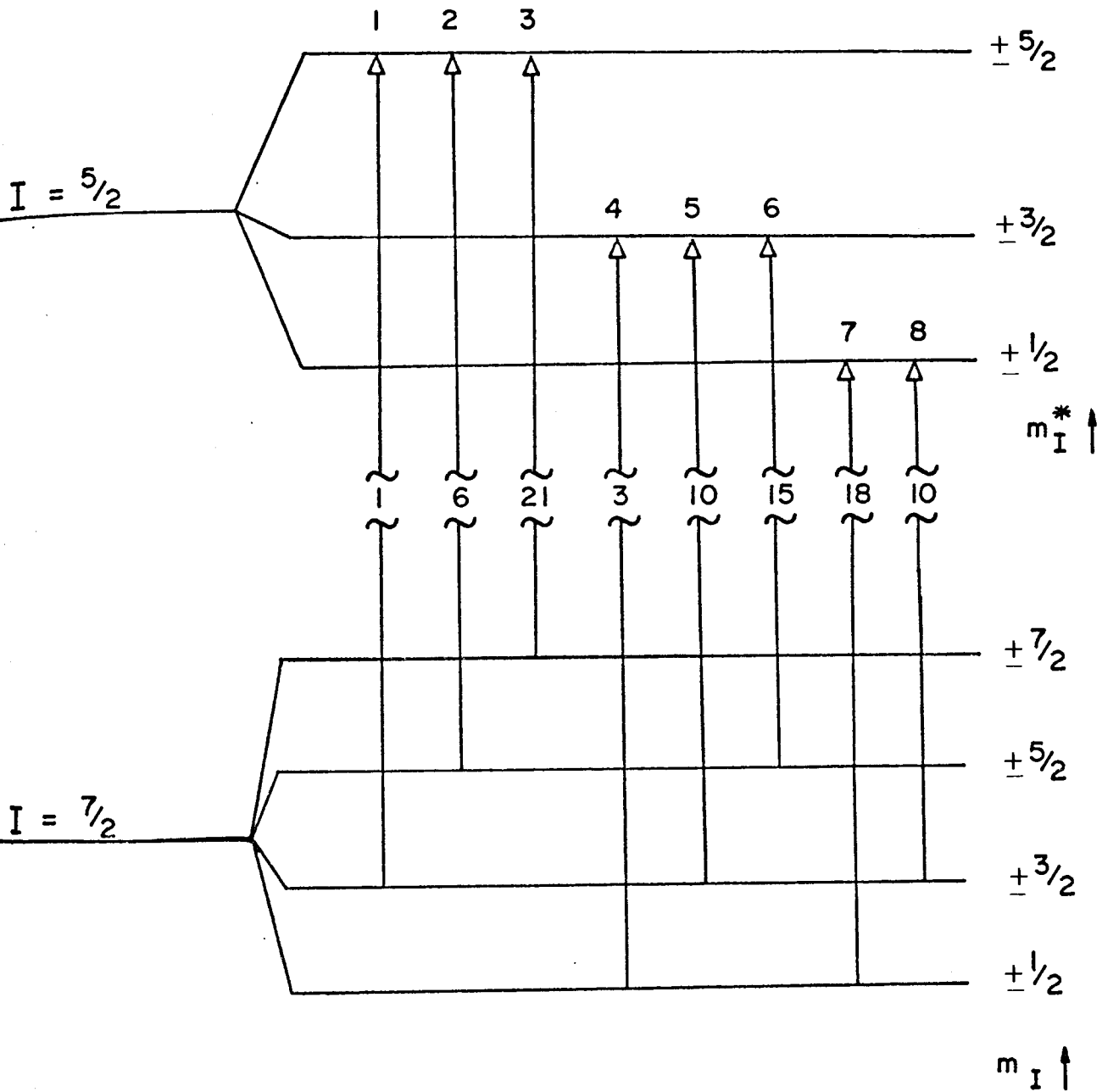


Figure 4. ^{129}I Quadrupole Splitting for e^2qQ_{nd} .
 Positive Clebsh-Gordon Coefficients, $\widetilde{\text{CG}}^2$,
 Are Given Showing the Relative Tran-
 sition Probabilities.

$$\delta = 2.23 \times 10^{-23} \frac{\delta R}{R} [|\psi_s(0)|^2_a - |\psi_s(0)|^2_s] \quad (V-1)$$

where $\frac{\delta R}{R} = +3 \times 10^{-5} [23]$. (V-2)

As for ^{125}Te , the ^{129}I Mössbauer transition has a positive $R_{ex}-R_{gnd}$ and thus a negative isomer shift corresponds to a lower $|\psi_s(0)|^2$ in the absorber than in the source, and a positive isomer shift a higher $|\psi_s(0)|^2_a$.

In Figure 5 is presented the isomer shift data reported in the literature for ^{129}I . Those compounds with $-\delta$ have relatively low $|\psi_s(0)|^2$ and this may be explained in terms of hybridization involving the $5s^2$ electrons on the iodine. In those compounds with $+\delta$, the $5s^2$ electrons on the iodine may be considered as a "lone pair". Removal of p-electrons in bonding leads to deshielding, and increasing $|\psi_s(0)|^2_a$. The removal of p-electrons from the iodine is linearly related to the isomer shift in these compounds by [26]:

$$\delta \text{ (mm. sec.}^{-1}\text{)} = 1.5 \text{ hp} - 0.54 \quad (V-3)$$

where hp is the number of p-electron holes in the $5p^6$ shell of iodine (I^- has hp = 0) and δ is measured relative to a ZnTe source.

As a result of the large electronegativity

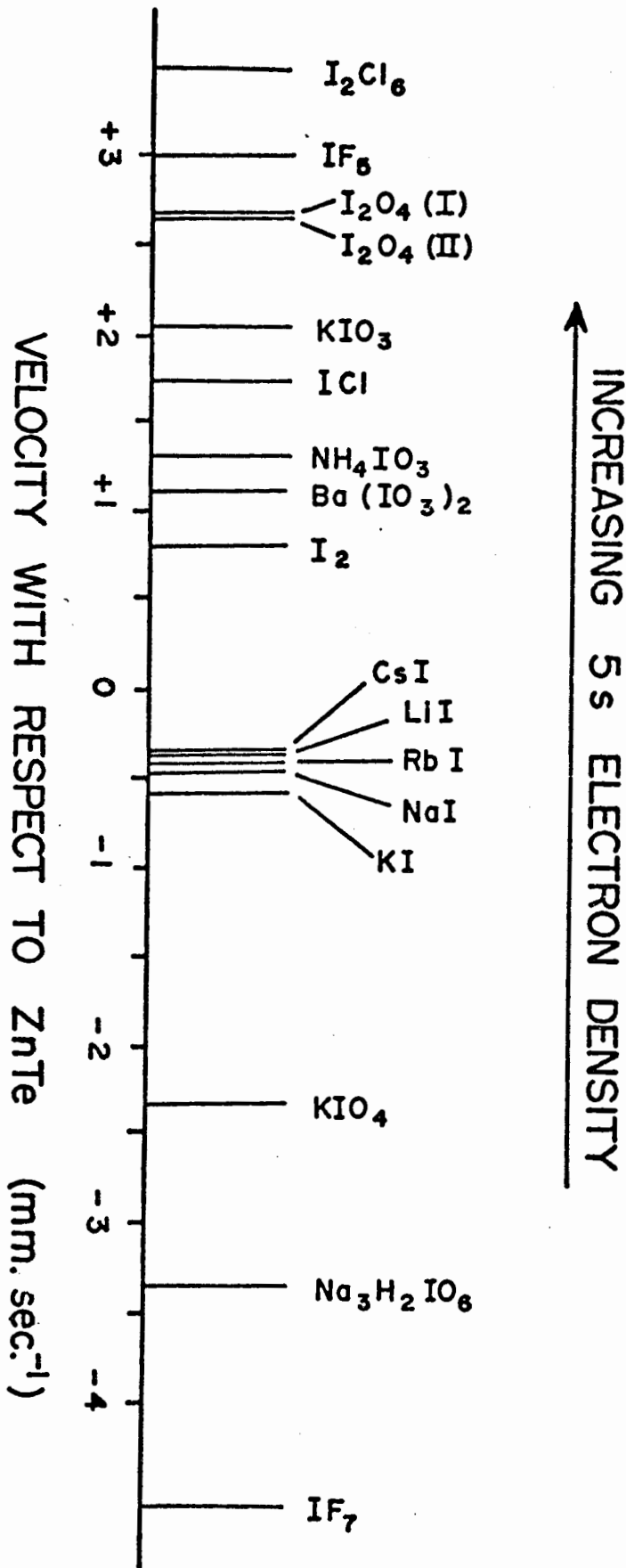


Figure 5. A Comparison of Isomer Shifts for ¹²⁹I - Labelled Iodine Compounds. A Positive Velocity Corresponds to the ZnTe Source Moving Towards the Absorber.

difference between iodine and fluorine, s-electrons participate in the bonding of IF_7 and IF_5 ^[24]. A term involving h_s , the number of s-electrons extracted from the $5s^2$ shell, must then be included in the expression $\delta = 1.5 h_p - 0.54$ ^[25, 26], to explain the Mössbauer isomer shifts in the analysis of the character of the I - F bond. The equation then becomes^[26],

$$\delta \text{ (mm. sec.}^{-1}\text{)} = -8.2 h_s + 1.5 h_p - 0.54. \quad (\text{V-4})$$

However the isomer shift could be affected by d-electron participation in the molecular orbitals of IF_5 and IF_7 , a point which has been neglected in this simple approach.

B. Quadrupole Coupling.

The theory used to interpret ^{129}I Mössbauer quadrupole coupling data was first proposed by Townes and Dailey^[27] to analyse nuclear quadrupole resonance (N.Q.R.) data. However this analysis can be carried further with ^{129}I Mössbauer than with N.Q.R. since the sign of the quadrupole coupling can also be obtained.

According to the theory of Townes and Dailey, the electrostatic field gradient, q_{molecule} , arises from an imbalance in the population of p orbitals in the molecule and can be related to that for an atom with just one hole in

its p shell, q_{atom} by

$$q_{\text{molecule}} = -U_p q_{\text{atom}} \quad (\text{V-5})$$

$$\text{where } U_p = -U_z + \frac{1}{2}(U_x + U_y) \quad (\text{V-6})$$

is the p-electron deficit or excess along the z axis.

U_x , U_y and U_z are the p-electron populations in the p_x , p_y , and p_z orbitals, with the principal axis of the molecule being defined as the z-axis. The description of the e^2qQ and η in terms of the p-electron distribution then becomes

$$e^2q_{\text{molecule}}Q = -U_p e^2q_{\text{atom}}Q \quad (\text{V-7})$$

$$\text{and } \eta = \frac{3}{2} \frac{U_x - U_y}{U_z} \quad (\text{V-8})$$

The value for $e^2q_{\text{at.}}Q$ for ^{129}I , as deduced from nuclear quadrupole resonance studies, is $-1607 \text{ Mc. sec.}^{-1}$. The experimental measurement of $e^2q_{\text{molecule}}Q$ and η do not alone allow the determination of U_x , U_y and U_z . However for the case of pure p bonding:

$$hp = 6 - (U_x + U_y + U_z) \quad (\text{V-9})$$

where hp can be obtained from δ as previously described.

Thus the values determined for U_x , U_y , and U_z will provide a fairly detailed picture of the distribution of p-electrons in the molecule.

A number of calculations of this sort have recently been reported on the iodine compounds ICl , IBr , I_2Cl_6 , $\text{I}_2\text{Cl}_4\text{Br}_2$ [24,28], I_2 [26], IF_5 , IF_7 [24], CH_3I , CH_2I_2 , CHI_3 , ClI_4 [29,30], SnI_4 [31, 32], ICN [33], and $(\text{NH}_4)_2\text{TeI}_6$ [34,35].

VI. ^{127}I Mössbauer.

The Mössbauer effect of the 57.6 keV. 1.9 nano-second transition in the ground state of ^{127}I (Figure 6) which follows the beta decay of $^{127\text{m}}\text{Te}$ has been used to measure the isomer shifts of a variety of compounds at 4.2°K. [4,36]. Although the quadrupole coupling constants for the ^{127}I nuclei are slightly greater than those for ^{129}I nuclei in the same chemical environment, the very broad natural line width, $2\Gamma = 2.54 \text{ mm. sec.}^{-1}$ and small isomer shifts of these spectra make them hard to resolve. For this reason ^{127}I Mössbauer spectra were not studied in the present work.

The experimentally measured isomer shift and quadrupole coupling ratios previously reported in the literature

$$\frac{\delta(^{129}\text{I})}{\delta(^{127}\text{I})} = -2.67 [37] \quad (\text{VI-1})$$

$$\frac{e^2qQ(^{129}\text{I})}{e^2qQ(^{127}\text{I})} = 0.70121 [38] \quad (\text{VI-2})$$

allows a comparison of ^{129}I Mössbauer parameters with ^{127}I Mössbauer and nuclear quadrupole resonance experiments.

This ratio may be compared to isomer shift ratios previously reported in the literature

$$\frac{\delta(^{129}\text{I})}{\delta(^{125}\text{Te})} = 3.15 \quad [39] \quad (\text{VI-3})$$

$$\frac{\delta(^{125}\text{Te})}{\delta(^{129}\text{I})} = 0.29 \pm 0.03 \quad [40] \quad (\text{VI-4})$$

These comparisons are developed further in the discussion.

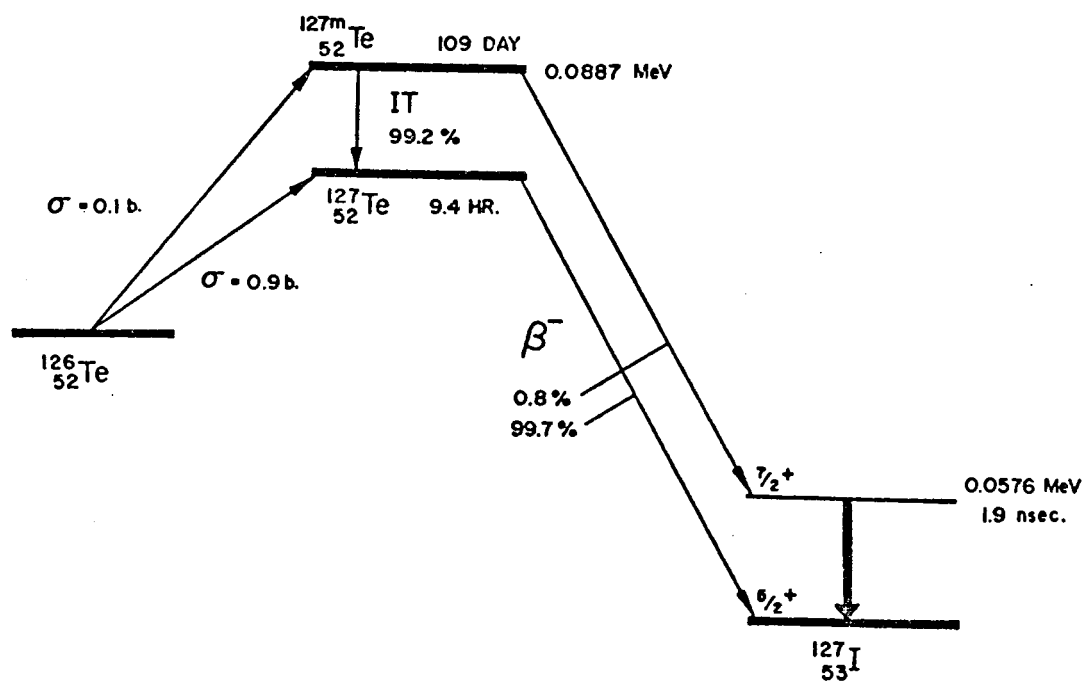


Figure 6. Decay Scheme Showing the Population of the Mössbauer Transition in ^{127}I .

VII. Nuclear Quadrupole Resonance Spectroscopy.

Pure quadrupole resonance, or nuclear quadrupole resonance spectroscopy (N.Q.R.), provides information about the electronic structure of chemical bonds analogous to that derived from Mössbauer spectroscopy. N.Q.R. measurements have been made previously on the tellurium hexahalides, TeX_6^{2-} ($\text{X} = \text{Cl}, \text{Br}, \text{I}$)^[41, 42, 43, 44, 45], tellurium tetrachloride TeCl_4 ^[46] and α dimethyl-tellurium dichloride^[47]. Other relevant compounds which have been studied include the interhalogens ICl_2^- , ICl_4^- ^[48, 49], I_2Cl_6 ^[50], IBr_2^- ^[51] and I_3^- ^[51, 54].

Only those isotopic nuclei which have a nuclear spin $I \geq 1$ possess a measurable nuclear quadrupole moment Q . Table I shows the halogens which have an electric quadrupole moment and are accessible to study through N.Q.R. spectroscopy.

TABLE I

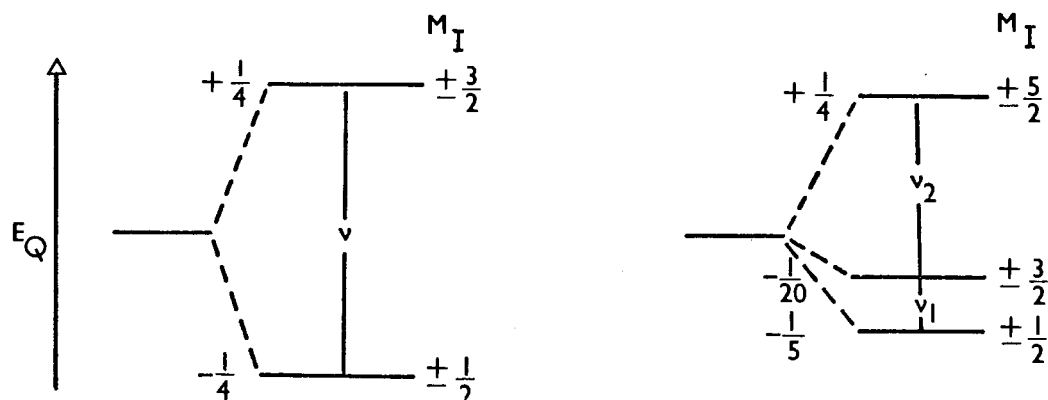
Atomic Quadrupole Coupling Constants eQq Atom of Halogens^a

<u>Nucleus</u>	<u>Spin I^b</u>	<u>$\frac{1}{2}eQq$ atom (Mc/sec.)</u>
^{35}Cl	3/2	-54.873 ± 0.005
^{37}Cl	3/2	-43.255 ± 0.005
^{79}Br	3/2	$+384.878 \pm 0.008$
^{81}Br	3/2	$+321.516 \pm 0.008$
^{127}I	5/2	-1146.356 ± 0.010

a Q is negative for Cl and I.^[16]

b It should be noted that the iodine isotopes are designated ^{127}I , ^{129}I etc., while I on its own is the general symbol for nuclear spin.

The energy diagrams for nuclei having an electric quadrupole moment of $\pm 5/2$ and $\pm 3/2$ placed in an inhomogeneous electric field are shown below.



A. N.Q.R. of Tellurium Compounds.

Townes and Dailey^[27] obtained relationships on bonding from N.Q.R. measurements for diatomic molecules in terms of a simple theory. They have shown that the quadrupole coupling constant of the halogen can be related to the covalent character (1-i) of the bond involving the halogen atom:

$$eQq_{\text{molecule}} = (1-i) (1-s) eQq_{\text{atom}}$$

where "i" denotes the ionic character of the bond and "s" is the s-character employed by the halogen in bonding.

The net charge, ρ , on the central atom is then

calculated to be

$$\rho = 4 - 6(1-i) \quad (\text{VIII-1})$$

for Te in TeY_6^{2-} . Calculations for several polyatomic molecules have been carried out [41, 44, 47, 55] which has extended this theory to certain special cases. In particular Nakamura et al. [41] have studied the halogen N.Q.R. spectra of TeY_6^{2-} ions and this work will be presented in some detail in the discussion.

Also the results of the N.Q.R. experiment carried out for TeCl_4 [46] agree quite well with the crystal structure of this compound since the six lines observed correspond to the slightly different environments of the six chlorine atoms surrounding the octahedrally co-ordinated tellurium. The crystal structure of TeCl_4 is discussed in detail in a later section.

B. N.Q.R Studies on Polyhalogens.

Yamasaki and Cornwell [48, 49] carried out N.Q.R. measurements on both the iodine and ligand chlorine in the crystalline compounds ICl , ICl_2^- , ICl_4^- and I_2Cl_6 . Their results suggested that d orbitals are considerably less important in bonding these compounds than had previously been supposed and that the p-bonding model proposed by

Pimentel^[57] represented a better approximation than the spd hybridization model. The N.Q.R. measurements also verified the prediction that the iodine coupling constants calculated for ICl_2^- and ICl_4^- are the same as that of ICl except for a change in sign in the case of ICl_4^- . This is consistent with a p-bonded model because in the case of ICl there is one short covalent bond while in the linear ICl_2^- ion the two long ionic bonds have the same net effect on the electrostatic field gradient at the iodine. In the case of the square planar ICl_4^- ion there are two p orbitals involved in bonding and one "lone pair" of electrons. In ICl_2^- there are two "lone pairs" and one p orbital involved in bonding, (Figure 7), so that the quadrupole coupling constants on the central iodine should be equal in magnitude but opposite in sign. This observation was born out experimentally through Mössbauer and N.Q.R. measurements^[4, 48, 49]. Yamasaki and Cornwell also calculated the electron distributions using a L.C.A.O. - M.O. approach. It was found that the general features of the electron distribution obtained were not markedly different assuming an s-character of the chlorine σ orbital in the range 0.0 - 0.3.

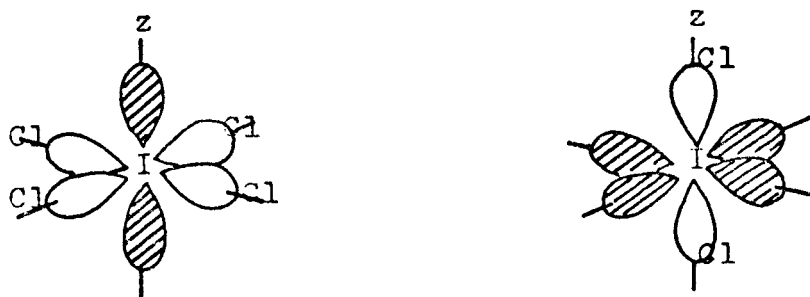


Figure 7. Orbital Populations in ICl_4^- and ICl_2^-

VIII. The Structures and Properties of the Tellurium Halides and the Polyhalogen Compounds.

A. Tellurium Halides.

1. Hexahalides.

Knowledge of the crystal structures of the tellurium compounds studied here will aid in bonding interpretations of Mössbauer data (Table II).

TABLE II

Crystal Structures of the Tellurium Halides *

Compound	Structure	Comments	Reference
$(\text{NH}_4)_2\text{TeCl}_6$	Cubic K_2PtCl_6	$\text{Te-Cl} = 2.541 \text{ \AA}$ TeCl_6^{2-} regular octahedron	58
$(\text{NH}_4)_2\text{TeBr}_6$	Cubic K_2PtCl_6 $T > 221^\circ\text{K.}$ distorted cubic $T < 221^\circ\text{K.}$ (probably tetragonal)	$\text{Te-Br} = 2.70 \text{ \AA}$ TeBr_6^{2-} regular octahedron	61
TeCl_4	$\text{Te}_4\text{Cl}_{16}$ units in a cubane-like structure	see Figure 8.	59, 60

$(\text{NH}_4)_2\text{TeCl}_6$ possesses the cubic K_2PtCl_6 structure with the TeCl_6^{2-} anion a regular octahedron^[58]. $(\text{NH}_4)_2\text{TeBr}_6$ also has the K_2PtCl_6 structure but becomes distorted at temperatures below 221°C ^[61] because the ammonium ion is smaller than the cavity formed by the twelve surrounding bromine atoms. However it was found that the regular octahedron of TeBr_6^{2-} is retained in both the K^+ and Cs^+

* covalent radii(\AA): Te-1.35; Cl-0.994; Br-1.142; I-1.333.
ionic radii(\AA): Cl-1.81; Br-1.95; I-2.16.

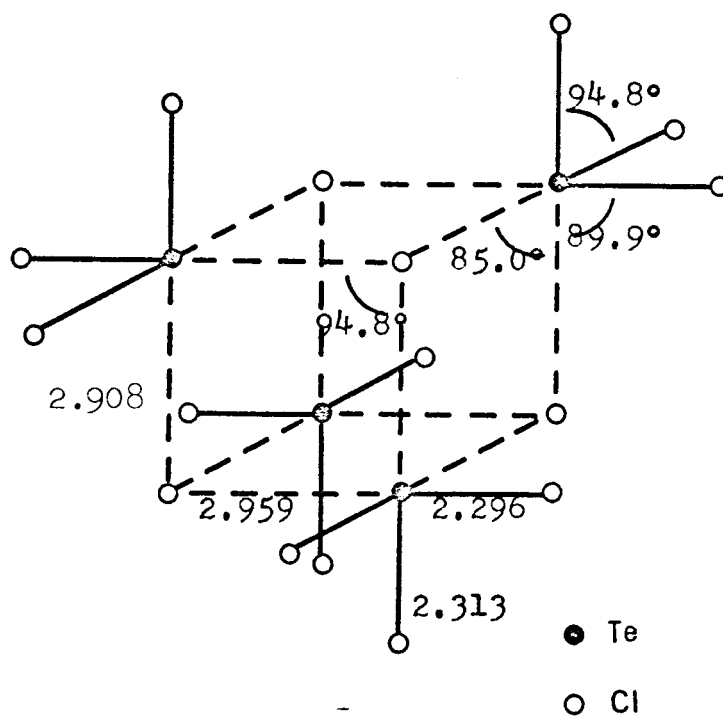


Figure 8. Crystal Structure of TeCl_4 [59,60]. The $\text{Te}_4\text{Cl}_{16}$ Molecular Unit (Two Fold Crystallographic Axis Vertical) is Shown With Some Individual Bond Distances in Å and Mean Values of Chemically Equivalent Bond Angles.

salts so that in these crystals the cation has little effect on the geometry of the anion.

The crystal structure of $(\text{NH}_4)_2\text{TeI}_6$ has not been reported, but Cs_2TeI_6 was found to possess the cubic K_2PtCl_6 structure^[62]. Therefore as in the hexabromide case, the $(\text{NH}_4)_2\text{TeI}_6$ probably possesses a distorted K_2PtCl_6 structure with the TeI_6^{2-} ion being a regular octahedron. The octahedral TeI_6^{2-} unit has also been reported in $\text{Mg}(\text{H}_2\text{O})_6\text{TeI}_6$ ^[63] and K_2TeI_6 ^[56].

The chemical stability of the TeX_6^{2-} anions with respect to total substitution, increases in going from Cl to I^[64]. This corresponds to an increase in covalent character of the Te-X bond as the electronegativity difference decreases between tellurium and halogen. N.Q.R. measurements^[41] have also demonstrated this.

2. Tetrahalides.

The crystal structure of TeCl_4 has been reported [59, 60]. TeCl_4 forms monoclinic crystals consisting of $\text{Te}_4\text{Cl}_{16}$ units (Figure 8). The shorter Te-Cl bond length corresponds to the sum of the covalent radii. Ionic bonding plays a more dominant role in the much weaker Te-Cl bridging bonds. This structure supports the model which suggests that the tellurium atom utilized 5p orbitals only, in bonding since all of the bond angles are $90^\circ \pm 5^\circ$. Each p orbital on the tellurium atom forms one short

covalent bond and one long ionic bond resulting in octahedral co-ordination. It is found that the Te-Cl bonds in the TeCl_3^+ group of TeCl_4 are much shorter than those of $\text{Te}^{\text{IV}}\text{-Cl}$ in $(\text{CH}_3)_2\text{TeCl}_2$ and TeCl_6^{2-} . In these latter compounds the same p orbital is probably bonding with two chlorine atoms thus resulting in two weak bonds with bond order of one-half. There is also evidence to suggest that the crystal structures of TeBr_4 and TeI_4 are similar to the structure of TeCl_4 . Crystal structure data on SeCl_4 , TeCl_4 and TeBr_4 [65] indicated that these molecules are isostructural. Blackmore et al. [66] prepared tetragonal crystals of TeI_4 , the structure of which was explained by considering an octahedral bond distribution for the tellurium atom. However two crystal forms of the tetraiodide are reported, the orthorhombic one being the more common.

Crystal data on SbCl_4^- , SbI_4^- , BiBr_4^- and BiI_4^- [67, 68], indicated that these ions exhibit octahedral co-ordination around the central metal atom with linking halogen bridges between metal atoms. Furthermore, there is little evidence for influence of the "lone pair" ^{*} of s-electrons in the above structures. Therefore it may be surmised that the TeX_4 (X = Cl, Br, I) compounds probably have octahedrally co-ordinated structures in the crystal similar to the iso-electronic bismuth and antimony halide ions for which the crystal structures have been reported.

* or "inert pair"

B. Polyhalogens.

The formation of the polyhalogens ICl_4^+ , IBr_4^+ , I_5^+ , ICl_6^- , IBr_6^- and I_7^- was expected to result from the beta decay of the tellurium halides. In this section the structure and stability of the known polyhalogens will be discussed.

Two classes of polyhalogen compounds exist: the interhalogen compounds are electrically neutral, and the polyhalides contain charged polyhalide ions (Table III). Wiebenga, Havinga and Boswyk^[69] have reviewed the extensive literature on the structures of the polyhalogen complexes. It appears that these structures are characterized by:

- (i) the presence of "polyvalent" halogen atoms,
- (ii) bond angles close to 90° or 180° and
- (iii) bond lengths which are some tenths of an angstrom longer than the sum of the covalent radii.

A more recent review by Wiebenga and Kracht^[70] describes the bonding in interhalogen compounds, polyhalide ions and positively charged polyhalogen ions by the use of a modified Hückel theory.

In this study we are particularly interested in the stability and structure of pentahalogens and heptahalogens. Crystal structures of the pentahalide ions ICl_4^- , BrF_4^- and I_5^- have been determined^[69].

TABLE III

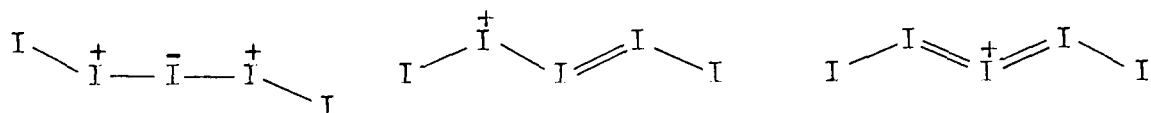
A. The Polyhalide ions [69-76].

I_3^-	I_2Cl^+	Br_5^-
I_2Br^-	I_2Br^+	BrF_4^-
I_2Cl^-	I_3^+	$I_2Cl_3^-$
IBr_2^-	Br_3^+	$I_2Cl_2Br^-$
$IBrCl^-$	I_4^{2+}	IF_4^+
$IBrF^-$	I_4^-	I_7^-
ICl_2^-	I_5^+	I_6Br^-
Br_3^-	I_5^-	IF_6^-
Br_2Cl^-	I_4Br^-	Br_6Cl^-
Cl_3^-	I_4Cl^-	I_8^{2-}
ClF_2^+	ICl_4^-	I_9^-
BrF_2^+	ICl_3F^-	Br_9^-
ICl_2^+	IF_4^-	I_{10}^-
		I_{11}

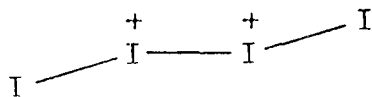
B. The Interhalogens [69, 77, 78].

IF	BrF_3	IF_5	IF_7
BrF	ClF_3	BrF_5	I_2Cl_6
ClF	Br_2Cl_2		
ICl	$BrCl_2^y$ ($y = Cl$ or Br)		
IBr			
BrCl			

In the first two cases, the ions have a square planar configuration with an iodine (or bromine) atom in the centre while in the latter case the iodine atoms form a "v" shaped ion and the structure can be described as consisting of an iodide ion to which two iodine molecules are attached. The difference in the two structures is also manifested by their difference in stability. In particular the ICl_4^- ion is characterized by its thermal stability while the I_5^- ion readily dissociates in solutions and upon heating. The mixed pentahalide ions I_2Cl_3^- and $\text{I}_2\text{Cl}_2\text{Br}^-$ [71] are also thought to have a structure similar to that of I_5^- . Plausible electronic structures and shapes have been proposed for I_5^+ as shown below. It was first detected by Gillespie and Milne [74, 79] in a solution of iodine oxidized by $\text{S}_2\text{O}_6\text{F}_2$ in fluorosulfuric acid.

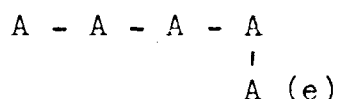
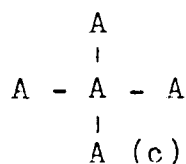
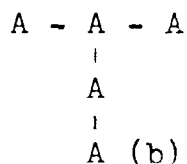
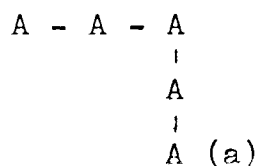


The I_2^+ and I_3^+ ions are also formed in the above solutions, [74, 79, 80], and on cooling the dimer I_4^{2+} is formed [76]. The tetrahedral and square planar structures for I_4^{2+} were eliminated in favour of the acyclic chain:



on the basis of a qualitative molecular orbital description of tetra-atomic molecules.

Delocalization energies for different possible configurations of a given number of halogen atoms have been calculated [69]. For the pentahalide ion it was shown that the arrangement represented in (a) below has the lowest energy in the first approximation using an L.C.A.O.-M.O. treatment.



However several T-shaped tetra-atomic molecules such as ClF_3 and BrF_3 [69, 70], have been discovered. Nelson and Pimental [78] also proposed the existence of several T-shaped molecules analogous to the fluorides possessing either the Cl-Br-Cl or the Cl-Br-Br unit.

In the compound $\text{N}(\text{C}_2\text{H}_5)_4\text{I}_7$ [69], no separate I_7^- ions can be distinguished. Centrosymmetrical I_3^- ions and I_2 molecules form a three dimensional pattern in which each I_3^- ion is surrounded by four I_2 molecules and each I_2 molecule is surrounded by two I_3^- ions. However the

distances between the I_3^- ions and I_2 molecules is smaller than the intermolecular spacing in crystalline iodine (3.56 Å) indicating a rather strong interaction. The compound I_8^{2-} has a linear structure similar to I_5^- .

It is found that the polyhalides are not stable with respect to dissociation into a monohalide and halogen or interhalogen compound^[69]. The dissociation always takes place in such a way that the halogen or interhalogen molecules formed contain the heaviest halogen atoms. This point must be remembered when interpreting the Mössbauer spectra of the polyhalide ions studied here.

Therefore, to date, no polyhalide ions with the molecular formula ICl_4^+ , IBr_4^+ , I_5^+ , ICl_6^- , IBr_6^- , and I_7^- have been synthesized by ordinary chemical methods.

IX Experimental.

A. The Mossbauer Spectrometer (Figure 9).

The Mössbauer experiments were carried out on an Nuclear Science and Engineering Corporation (NSEC) AM-1 drive system and cryoflask, used in conjunction with a Nuclear Data 2200 series 1024-channel analyser. Routine calibration of the spectrometer using standard $\text{Na}_2\text{Fe}(\text{CN})_5\text{NO} \cdot 2\text{H}_2\text{O}$ and $\alpha\text{-Fe}_2\text{O}_3$ absorbers [101] showed that the velocity scale was linear ($\pm 0.5\%$) over the velocity range used in this work and that the zero velocity channel was reproducible to within ± 0.2 channels. In general, sets of 2×256 channel mirror image spectra were obtained with the transducer operating at 25 cycles per second and an analyser multiscalar dwell-time of 80 microseconds per channel.

The cryoflask used with this system was a metal vacuum cryostat which held liquid nitrogen for ca. 35 hours, maintaining the source and absorber at 80°K. The cryoflask also held liquid helium for ca. 10 hours.

The Mössbauer source and absorber compounds were mixed with a small amount of silicon grease before being placed in the source or absorber holders. This was done firstly to give good thermal contact between the compound and secondly to evenly distribute the material over the holder ensuring uniform thickness.

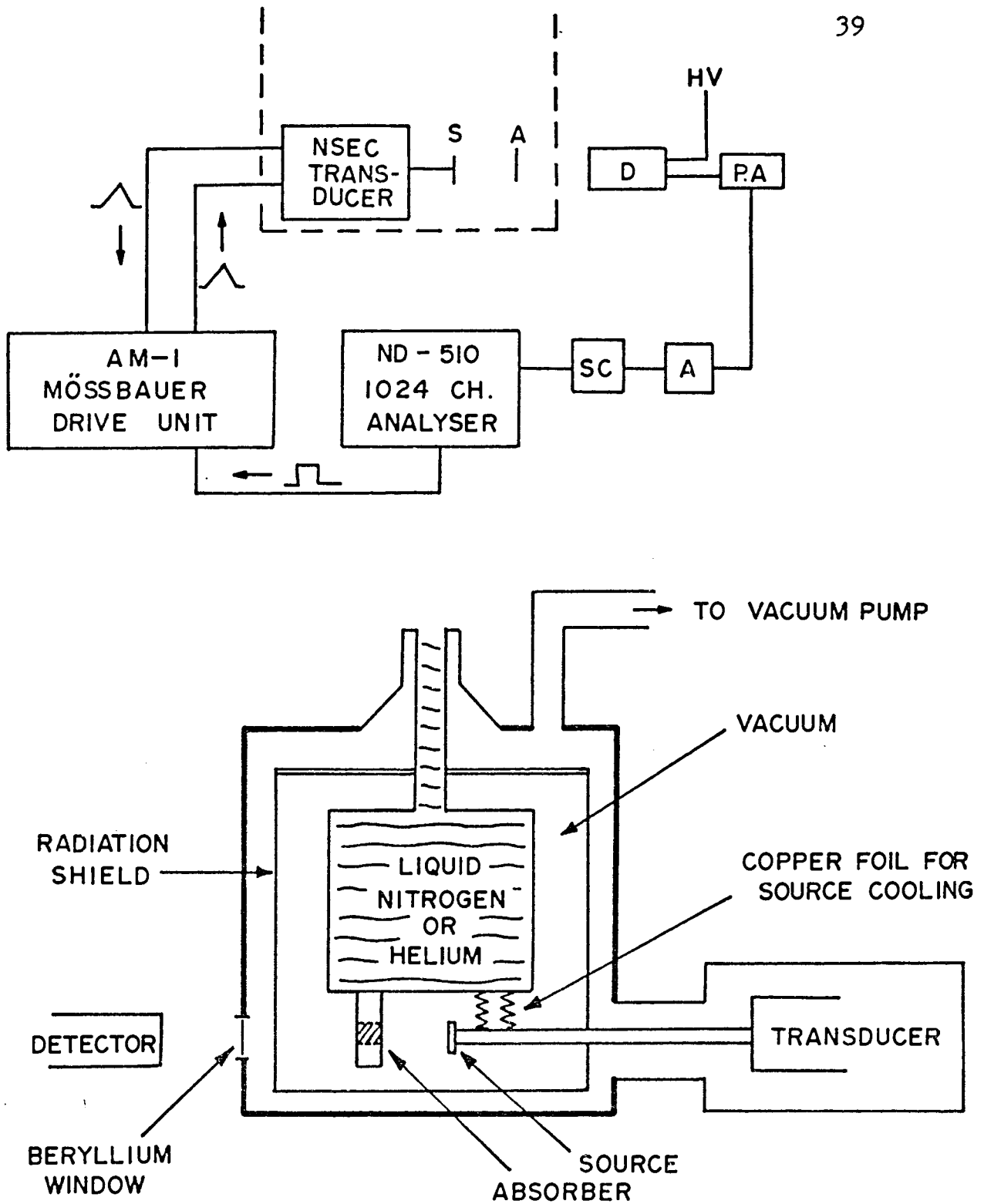


Figure 9. Diagram of the Mössbauer Spectrometer.

A teflon absorber holder with an o-ring seal was used to hold the absorber compounds studied [88].

B. Preparation of the Compounds.

The preparation of the parent tellurium compounds used in this study were carried out as reported in the literature.

The procedures are summarized below:

1. Te^{v}_4 , v = Cl, Br, I [81].

Tellurium metal was dissolved in $\text{HNO}_3/\text{H}_2\text{O}$ and the solution evaporated to dryness. While still hot the $\text{Te}_2\text{O}_4\text{HNO}_3$ residue was dissolved in the corresponding concentrated acid, HY. After cooling in ice, concentrated sulfuric acid was added to precipitate Te^{v}_4 , which was then filtered from the solution by suction.

2. TeI_4 .

As well as using the above method, TeI_4 can be prepared by two other methods [66, 82]:

(i) A Stoichiometric amount of tellurium and iodine in an evacuated sealed tube was heated at 500°C for eight hours.

(ii) TeI_4 was also prepared via telluric acid [83, 84]. Tellurium metal was dissolved in $\text{HNO}_3/\text{H}_2\text{O}$, and the tellurite ion formed then oxidized with potassium permanganate, with hydrogen peroxide being added to reduce the manganese dioxide formed. Addition

of concentrated nitric acid precipitated telluric acid, which was then filtered and washed with concentrated nitric acid. The telluric acid was then dissolved in concentrated hydriodic acid, and on slow evaporation, TeI_4 precipitated.

(iii) The absorber $\text{Te}^{129}\text{I}_4$ was also prepared. The Na^{129}I solution obtained from Oak Ridge was acidified with dilute nitric acid and the iodine was precipitated out of solution by adding an excess of a saturated solution of sodium nitrite. After centrifuging and removal of the mother liquor, the iodine was sublimed through calcium carbonate into a tube containing tellurium powder. The tube, evacuated and sealed, was heated to 500°C for eight hours to ensure complete reaction.

3. $(\text{NH}_4)_2\text{TeY}_6$ [85, 86].

As in the preparation for TeY_4 , tellurium metal was dissolved in $\text{HNO}_3/\text{H}_2\text{O}$ and the solution evaporated to dryness. While still hot, the residue was dissolved in the corresponding concentrated acid HY . A few drops of NH_4Y in concentrated HY precipitated out $(\text{NH}_4)_2\text{TeY}_6$.

4. ZnTe [87].

Zinc telluride was prepared by heating a stoichiometric amount of powdered tellurium and zinc in an evacuated silica tube at 750°C for several hours. This produced red, cubic ZnTe .

C. Raman Spectra and Elemental Analysis.

The Raman Spectra of TeY_4 and $(\text{NH}_4)_2\text{TeY}_6$ ($\text{Y} = \text{Cl}$,

Br) are summarized in Table IV along with the literature values. A Raman spectrum could not be obtained for the very darkly coloured TeI_4 and the assignment of the lines in the Raman spectrum of $(\text{NH}_4)_2\text{TeI}_6$ is very dubious.

TABLE IV

Raman Spectra of the Tellurium Halides

Compound	ν_1 (cm. ⁻¹)	ν_2 (cm. ⁻¹)	ν_3 (cm. ⁻¹)	Reference	
TeCl_4 (white solid)	375s ^a 376s 376s	348s 347s 351s	341s 343s	150w 150w	* 88 89
TeBr_4 (orange solid)	245s 250s	231s 226s	224s 220s	133vw 124vw 133vw 125vw	* 89
$(\text{NH}_4)_2\text{TeCl}_6$ (yellow solid)	299s 299s 300s	250s 241s 251s	143s 143s 145s	 53s	* 90 91
$(\text{NH}_4)_2\text{TeBr}_6$ (orange-red solid)	178s	155s	91w	75s	*
K_2TeBr_6	178s	155s	90w	70w	91
$(\text{NH}_4)_2\text{TeI}_6$ (dark red solid)		108, 74 and 59w			*
K_2TeI_6		105, 75 and 60w (assignment doubtful)			91

a s = strong, w = weak, vw = very weak.

* This work.

The elemental analysis results are in good agreement with the calculated values for tellurium and halogen content in all of the halides (Table V).

TABLE V

Elemental Analysis Results for Tellurium and Halogen Content

Compound	Calculated		Obtained ^b	
	Te	X ^a	Te	X
TeI ₄	20.09	79.91	19.79	79.80
(NH ₄) ₂ TeCl ₆	34.36	57.28	34.22	56.39
(NH ₄) ₂ TeBr ₆	20.00	75.14	20.16	74.44
(NH ₄) ₂ TeI ₆	13.87	82.77	13.98	82.14

a X = Cl, Br or I.

b Analysis carried out at Alfred Bernhardt Analytical Laboratory, West Germany. The analysis on TeCl₄ and TeBr₄ was not carried out because the samples were wet with sulfuric acid.

D. Mössbauer Experiments with ¹²⁵Te.

In characterizing the tellurium compounds used in this work, the ¹²⁵Te Mössbauer absorption spectra were measured and compared with those reported in the literature.

The features of the Mössbauer effect with ¹²⁵Te have been reported in several papers [10, 11, 18, 20, 92, 93].

The principle difficulty in detection of the 35.5 keV. gamma ray from the Mössbauer transition in ¹²⁵Te derives from the fact that this transition has a K-shell internal conversion coefficient of 11. This leads to a very high tellurium X-ray background (TeK_α = 27.4 keV, TeK_β = 31.2

keV.) which cannot be resolved from the Mössbauer transition. A Xe(CO₂) proportional detector was used because the energy of the K-absorption edge (34.51 keV.) is between ¹²⁵Te γ-ray and gamma ray energies. Thus, only the 35.6 keV. gamma ray is capable of K-shell photo-electric absorption and subsequent excitation of xenon γ-rays. The 6.9 keV. escape peak is counted in the Mössbauer experiment.

1. ¹²⁵I/Cu Source.

A 20 millicurie ¹²⁵I on copper source from New England Nuclear was used. The ¹²⁵I → ¹²⁵Te electron capture decay scheme is illustrated in Figure 1.

A five mm. thick copper absorber was placed immediately in front of the source and this reduced considerably the background under the 6 keV. escape peak in the detector. The 8 keV. copper γ-rays produced were efficiently absorbed in the absorber holder and the vacuum dewar window.

2. ¹²⁵Te Absorber Compounds.

The absorber compounds for ¹²⁵Te Mössbauer experiments were synthesized with tellurium metal enriched to 71.7% in ¹²⁵Te following the procedures outlined earlier.

F. Mössbauer Experiments with ¹²⁹I.

The ¹²⁹I Mössbauer spectra were recorded using a Harshaw NaI(Tl) γ-ray detector, integrally mounted on a

photo-multiplier tube, together with an Ortec model 113 preamplifier and model 440 A selective filter amplifier. When using ^{129m}Te sources, 27.47 keV. tellurium γ -rays are seen in all isomeric transitions feeding ^{129}Te . The pulse height analysis spectrum showed only a single broad peak, the 27.7 keV Mössbauer transition not being resolved from the γ -rays in the detector thus making the background count very high.

1. Source Activities for ^{129}I Emission Experiments.

The ^{129m}Te was obtained by the irradiation of 50 mg. amounts of 99.46% ^{128}Te metal in quartz ampoules for two weeks at c.a. 10^{14} n.cm.⁻²sec.⁻¹, in the N.R.U. reactor at Chalk River. The tellurium metal was then used in the preparation of the compounds described earlier. These sources generally ranged in activity from 0.5 to 2.0 mCi. and were usually less than 10 mg.cm.⁻² in thickness.

A preparative route applied by J. L. Warren [7] was used in the preparation of the ^{129}Te Mössbauer source. The isomer separation of ^{129}Te and ^{129m}Te was achieved through the chemical effects of the isomeric transition in solution. ^{129m}Te labelled telluric acid was dissolved in 4N HCl. In this solution the $^{129m}\text{Te} \rightarrow ^{129}\text{Te}$ isomeric transition produces bond rupture in more than 90% of events, giving $^{129}\text{Te}(\text{IV})$ in solution. In the presence of

Te(IV) carrier, SO_2 is bubbled through the solution, this selectively reducing the $^{129}\text{Te(IV)}$ to tellurium metal, the $^{129\text{m}}\text{Te}$ remaining in solution as $\text{H}_6^{129\text{m}}\text{TeO}_6$. The separated ^{129}Te labelled metal was then used in the immediate preparation of TeCl_4 .

2. Absorbers.

A Na^{129}I absorber sealed in a plastic cell was prepared by the **evaporation** of an aqueous solution of Na^{129}I obtained from Oak Ridge. It contained approximately 15 mg.cm.^{-2} of ^{129}I . This absorber was used in all $^{129\text{m}}\text{Te}$ emission experiments. It was confirmed as a single line absorber against a $\text{Zn}^{129\text{m}}\text{Te}$ source giving a line width of $1.25 \text{ mm.sec.}^{-1}$ at liquid nitrogen and 1.4 mm.sec.^{-1} at liquid helium temperatures. The experimental line widths in this work varied from 1.0 to 1.9 mm.sec.^{-1} at liquid nitrogen temperatures and from 1.5 to 3.8 mm.sec.^{-1} at liquid helium temperatures.

F. Computer Analysis of Mössbauer Spectra.

The Mössbauer spectra were fitted to Lorentzian curves by means of a computer analysis [100]. The program used required initial estimates of the line positions, full-widths, and intensities, and allowed for the constraining of any number of these parameters during the fitting procedure. In an ideal case, all such constraints

should be removed during the latter part of the computation. However, for the more complex ^{129}I spectra, some of which contained two superimposed 8-line quadrupole split spectra, it was found necessary to constrain many of the absorption line parameters throughout the fitting process. The program gave a value of chi-squared, χ^2 , for each fit, which allowed a ready assessment of the statistical acceptability of the fit. Only when the $\frac{\chi^2}{N}$ value indicated a degree of confidence less than the 0.1% point, that is $\frac{\chi^2}{N} < 1.3$, was the computer fit of a spectrum judged to be acceptable. Here N is the number of degrees of freedom.

All of the spectra obtained in this work were mirror-image spectra and the two halves were always computed separately.

v. Results.

A. ^{125}Te Absorption Spectra.

The ^{125}Te Mössbauer absorption spectra were recorded at 80°K relative to an $^{125}\text{I}/\text{Cu}$ source. The quadrupole splittings and isomer shifts are reported in Table VI. The data are compared with several values previously reported in the literature. Representative spectra are shown in Figure 10.

It can be seen that the isomer shifts for the TeV_6^{2-} compounds are in good agreement with Gukasyan et al. [95] but in poor agreement with Gibb, et al. [93]. Erickson and Maddock [96] have noted that the isomer shift data reported by different laboratories for the same compounds show a wide range of values, presumably as a result of different source preparations. Another source of error may be the incorrect reporting of the standard for the isomer shift. Thus Gibb et al.'s data shows a consistent trend to more positive isomer shifts than those of other workers. This may be explained in part, if their data are quoted with respect to $\delta_{\text{ZnTe}} = 0$ rather than with respect to an $^{125}\text{I}/\text{Cu}$ source.

The isomer shift values for the TeV_4 compounds are in agreement with those reported by Jung and Triftshäuser [11] but differ from those of Unland [92], although the statistical accuracy of the results of the last workers was very poor.

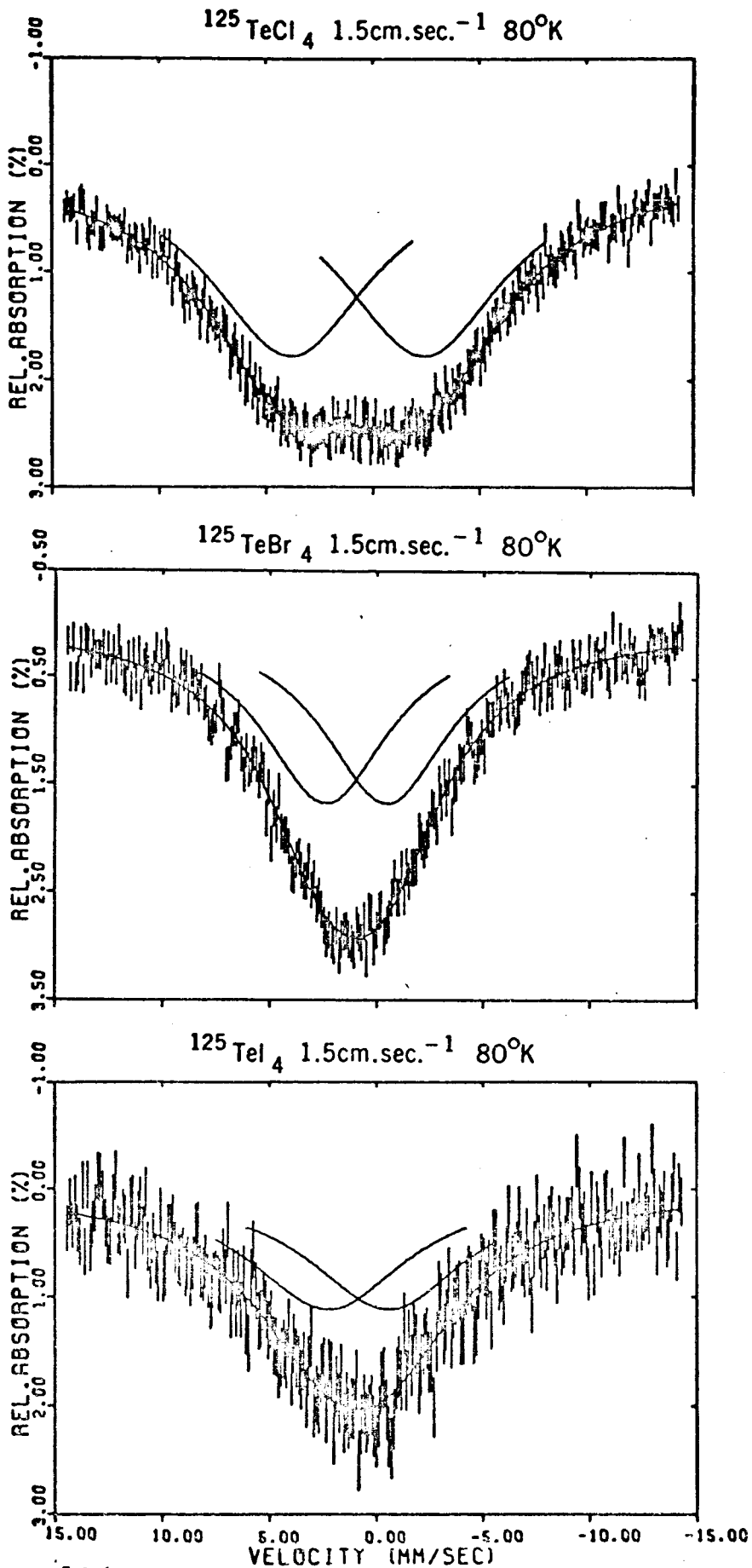


Figure 10. ^{125}Te Absorption Spectra of the TeX_4 ($X = \text{Cl}, \text{Br}, \text{I}$) Compounds.

TABLE VI

 ^{125}Te Mössbauer Absorption Parameters.

	$^{125}\delta^a$	Δ^b	Reference
	mm. sec. ⁻¹	mm. sec. ⁻¹	
TeCl_4	$+1.0 \pm 0.3$	6.0 ± 0.2	*
	$+1.2 \pm 0.1$	4.0 ± 1.6	11
	$+2.7 \pm 0.4$	5.4 ± 0.8	92
TeBr_4	$+1.1 \pm 0.2$	2.8 ± 0.2	*
	$+1.1 \pm 0.1$	3.8 ± 4.0	11
	$+1.6 \pm 0.3$	5.0 ± 1.4	92
TeI_4	$+1.0 \pm 0.2$	2.7 ± 1.0	*
	$+1.8 \pm 0.9$	4	11
	$+1.0 \pm 0.6$	6.0 ± 1.0	10
$(\text{NH}_4)_2\text{TeCl}_6$	$+1.7 \pm 0.1$	0.0	*
	$+1.70 \pm 0.05$	0.0	95
	$+1.95 \pm 0.05$	0.0	93
$(\text{NH}_4)_2\text{TeBr}_6$	$+1.4 \pm 0.1$	0.0	*
	$+1.52 \pm 0.05$	0.0	95
	$+1.73 \pm 0.04$	0.0	93
$(\text{NH}_4)_2\text{TeI}_6$	$+1.1 \pm 0.1$	0.0	*
	$+1.24 \pm 0.08$	0.0	95
	$+1.54 \pm 0.09$	0.0	93
ZnTe	-0.07 ± 0.07	0.0	94

a with respect to an $^{125}\text{I}/\text{Cu}$ source.

b Conversion into $e^2qQ(1 + \eta^2/3)^{1/2}$ in Mc. sec.⁻¹ is obtained by multiplying by 57.4.

* This work

The % resonance absorptions for the spectra were small, reflecting small recoil-free fractions in these compounds. This is due to the low rigidity of the tellurium halide lattices (evidenced by their low melting points), along with the high energy, 35.5 keV., of the Mössbauer gamma ray. An experiment on $^{125}\text{TeCl}_4$ at liquid helium temperature produced a marked increase in the % resonance absorption (to 12%), but lead to a loss in resolution in the spectrum through line broadening. This was a significant disadvantage in measuring the very small Δ in the TeX_4 compounds. Therefore all measurements were made at 80°K.

B. ^{129}I Emission Spectra.

All spectra were recorded at 4°K and also at 80°K where the % resonance absorption was large enough to be distinguished from the background. These emission spectra were recorded against a single-line Na^{129}I absorber which had been independently calibrated using a $\text{Zn}^{129\text{m}}\text{Te}$ source. The ^{129}I isomer shifts and quadrupole couplings obtained for the compounds investigated in the work are shown in Table VII. To allow a ready comparison of the data with the absorption values for ^{129}I compounds reported in the literature, all the emission data has been corrected to correspond to that for an absorption experiment relative

to a ZnTe source. To achieve this correction for the isomer shifts the following relationship was used:

$$\text{reported } \delta = -(\text{experimentally observed } \delta + 0.46) \text{ mm. sec.}^{-1}$$

(X-1)

where $+0.46 \text{ mm. sec.}^{-1}$ is the isomer shift for a Na^{129}I absorber relative to a ZnTe source (Table VII).

The quadrupole coupling measurements were corrected by changing the sign. The emission spectra shown in Figures 11 - 15 are the experimentally recorded spectra without conversion into absorption parameters.

1. Emission Spectra of the $(\text{NH}_4)_2^{129\text{m}}\text{TeX}_6$ Compounds.

Initially the emission spectra for all three compounds were measured at 80°K as shown in Figure 11(b) for $(\text{NH}_4)_2\text{TeBr}_6$. Very small % resonance absorptions were observed, particularly in the case of $(\text{NH}_4)_2\text{TeI}_6$. Measurements were then made at 4°K and the spectra are shown in Figures 12 and 13. As can be seen, an increase in the % absorption was observed. Moreover, in the $(\text{NH}_4)_2\text{TeCl}_6$ and $(\text{NH}_4)_2\text{TeBr}_6$ sources, in addition to the single intense line of large isomer shift observed at 80°K , additional lines of relatively low intensity were observed at 4°K (Figure 11). For the $(\text{NH}_4)_2\text{TeI}_6$ source these other lines appeared to dominate the spectrum (Figure 13).

TABLE VII

$(\text{NH}_4)_2\text{TeX}_6$ Mössbauer Emission Experimental Data.

Compound	Temp.		$129\delta_a$		e^2qQ^a		η	Intensity % ^b	$\frac{\chi^2}{N}$
	°K.	mm. sec. ⁻¹	mm. sec. ⁻¹	Mc. sec. ⁻¹	Mc. sec. ⁻¹				
$(\text{NH}_4)_2^{129\text{m}}\text{TeCl}_6$	80	$6.09 \pm .15$		0	0	0	0	80	1.14
	4	$6.23 \pm .08$		0	0	0	0	80	1.23
$(\text{NH}_4)_2^{129\text{m}}\text{TeBr}_6$	80	$5.08 \pm .01$		0	0	0	0	80	0.63
	4	$5.08 \pm .09$		0	0	0	0	80	0.96
$(\text{NH}_4)_2^{129\text{m}}\text{TeI}_6$	4	$3.56 \pm .08$		0	0	0	0	16	0.92
		$1.9 \pm .4$		-1200 ± 100	$0.3 \pm .2$				

a. δ and e^2qQ are relative to a ZnTe source in an absorption experiment.

b. Intensity expressed as a % of the total resonance absorption observed.

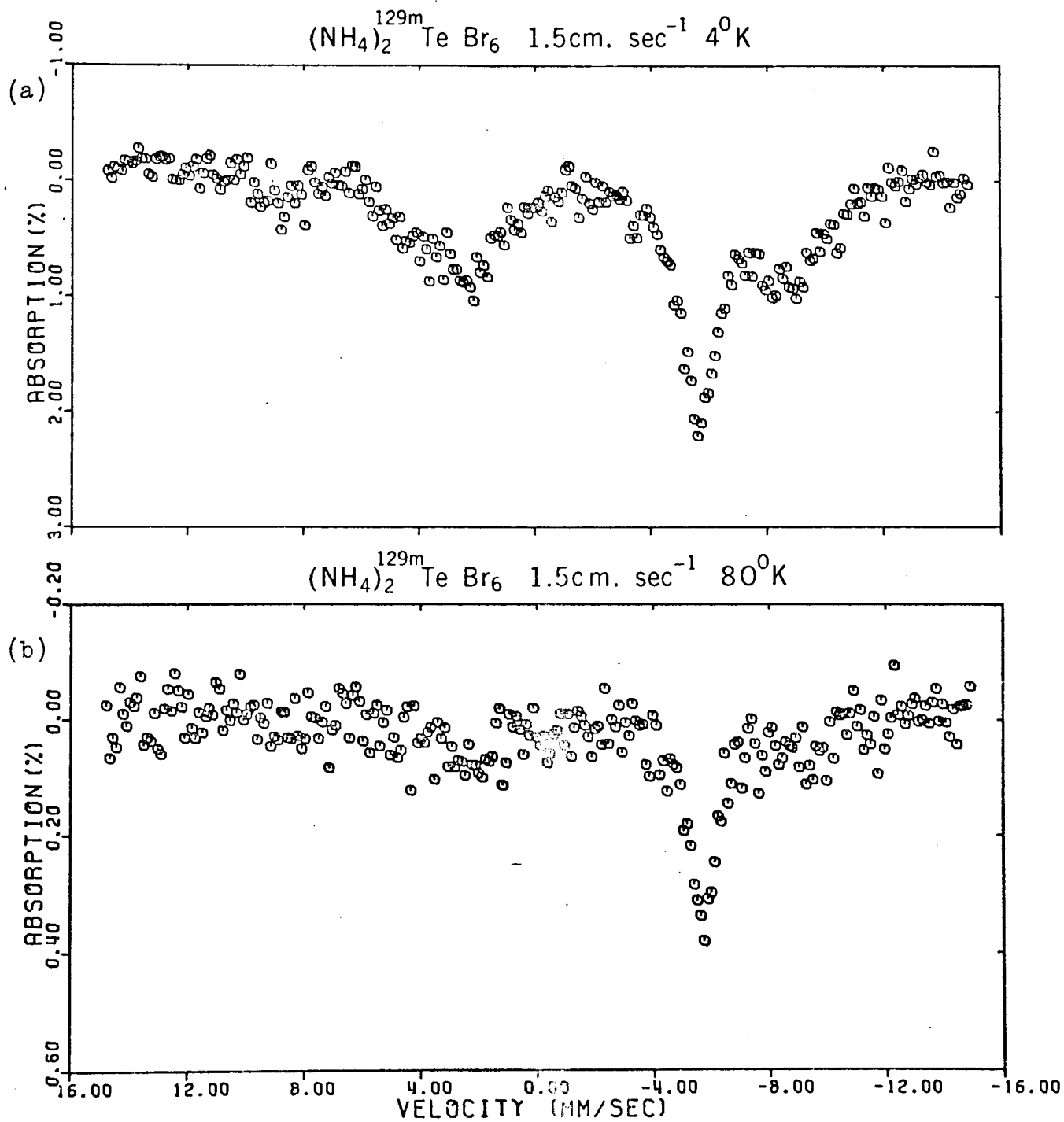


Figure 11. ^{129}I Mössbauer Emission Spectra of $(\text{NH}_4)_2\text{TeBr}_6$.

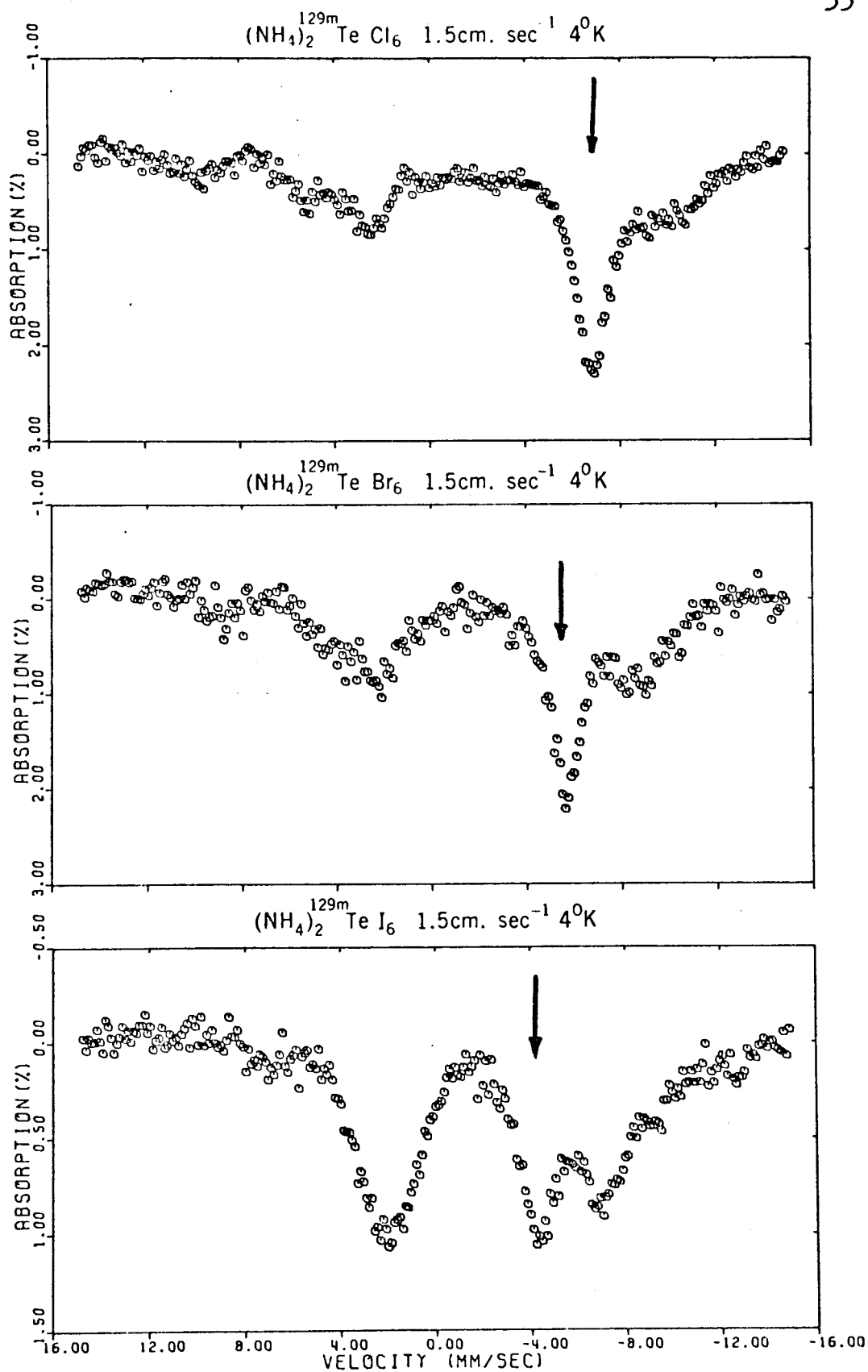


Figure 12. ^{129}I Emission Spectra of the $(\text{NH}_4)_2\text{TeX}_6$
 (X = Cl, Br, I) Compounds.

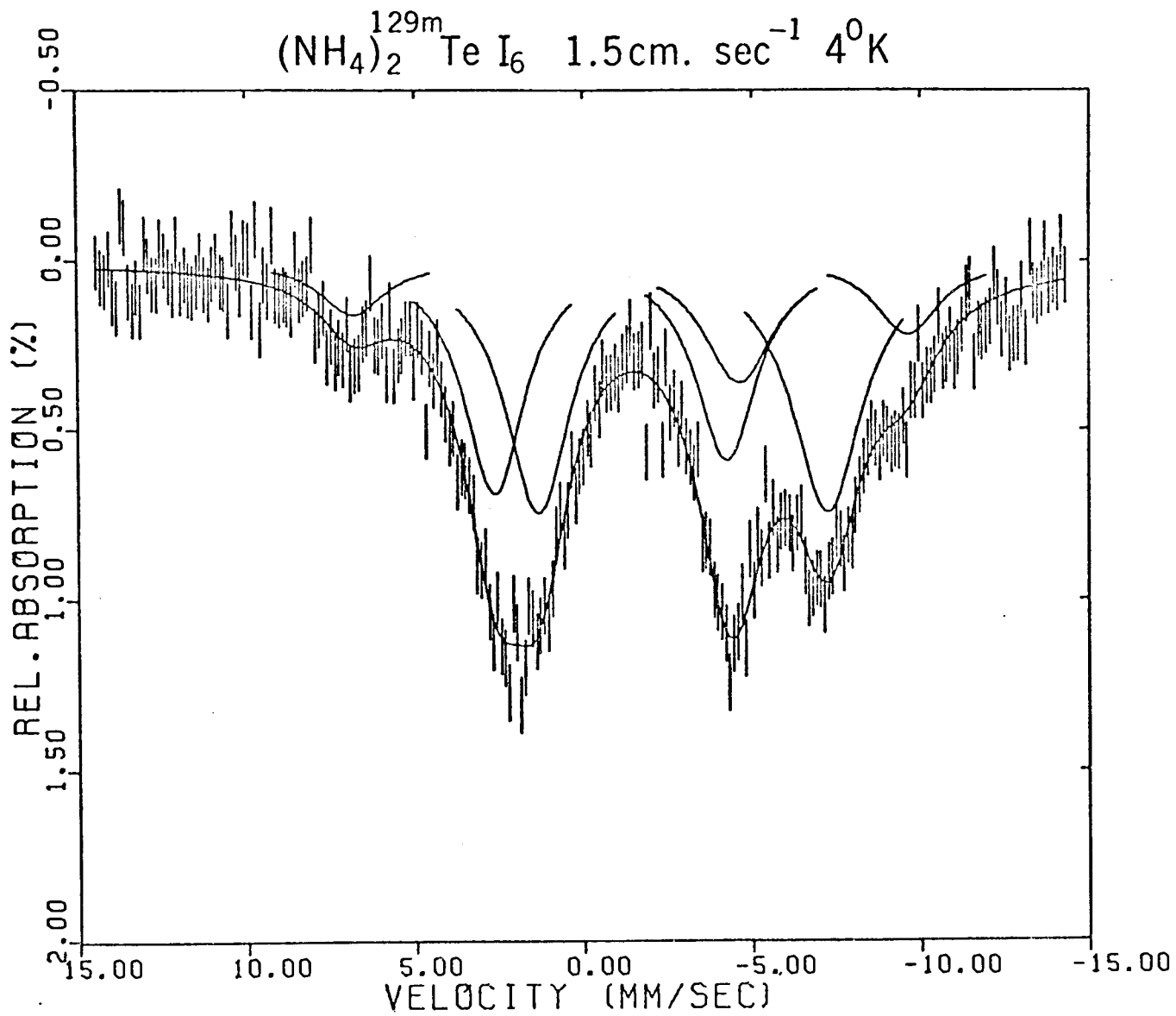


Figure 13. $^{129\text{m}}\text{I}$ Emission Spectrum of $(\text{NH}_4)_2\text{TeI}_6$.

In each of the spectra at 4°K it is possible to identify a single line of large isomer shift which is assigned to the IX_6^- ion in each case (Figure 12). The evidence which supports this conclusion will be presented in detail in a later section. The isomer shifts for the postulated IX_6^- anions are shown in Table VII. The additional lines observed in each spectrum may have their origin in

(i) impurities present in the source sample,

(ii) decomposition products formed in the $^{129\text{m}}\text{Te}$ ^{129}Te isomeric transition preceding the beta decay.

or

(iii) decomposition products resulting from the instability of the $^{129}\text{IX}_6^-$ ions themselves.

The chemical analyses of the compounds gave no evidence of macroscopic amounts of impurities. Moreover, repeated preparations of each source compound gave essentially identical results for any one compound. The second possibility listed could have been checked had it been possible to study ^{129}Te labelled sources where the effects of the isomeric transition would no longer be present. This study was not possible because of the 69 minute half-life of this isotope, together with the time taken to prepare the compounds, mount them in the dewar and cool the experimental apparatus to 4°K.

A further point which is relevant to the presentation of the experimental results is the measured linewidths in the emission spectra, which ranged from 1.5 through 1.7 to 2.3 mm.sec.⁻¹ for the ICl₆⁻, IBr₆⁻ and II₆⁻ ions respectively. These compare with a natural linewidth for the transition of 0.59 mm.sec.⁻¹. The observed line-broadening could not have arisen exclusively from the absorber or source thickness or from mechanical vibrations due to liquid helium boil-off, since the linewidth of the Na¹²⁹I absorber recorded against a Zn^{129m}Te source of similar mass was found to be 1.25 mm.sec.⁻¹ at 80°K and 1.4 mm.sec.⁻¹ at 4°K. The other likely causes of line-broadening may be listed as:

(i) decomposition of the ¹²⁹IX₆⁻ ion over the lifetime of the Mössbauer transition which would shorten the effective half-life of the state [97].

(ii) a spectrum of isomer shifts and/or quadrupole splittings arising from a spectrum of lattice sites which the ¹²⁹I impurity atoms may occupy in the crystal.

(iii) crystal distortions at 4°K which may give rise to small quadrupole splittings; (such distortions have been reported in the X-ray crystal studies of TeBr₆²⁻ (Table II)).

The results of the present experiments do not allow us to distinguish between these several possibilities. It may be noted however that line-broadening is generally observed in emission spectra and no firm explanation has yet been offered to explain this phenomenon.

2. Emission Spectra of the $^{129m}\text{TeY}_4$ Compounds.

With the $^{129m}\text{TeY}_4$ sources (Y=Cl, Br, I) no measureable resonance absorption was observed at 80°K. Thus all three compounds were studied at 4°K (Figure 14). Even at 4°K only about 1.5% absorption was observed and this, coupled with broad linewidths, resulted in very poorly resolved spectra.

Following a detailed examination of these spectra it was firmly concluded that the ^{129}I daughter atom was not present in a lattice environment isoelectronic or isostructural with that of the parent, i.e. molecular rearrangement or decomposition appeared to accompany the $^{129}\text{Te} \rightarrow ^{129}\text{I}$ decay in all events. Again, the detailed arguments supporting the conclusion will be presented later. The TeY_4 emission spectra were computer fitted and a statistically acceptable fit obtained assuming the presence of a single quadrupole split species with a large quadrupole coupling constant and one additional single line (Figure 14). The computed parameters for the quadrupole split and the single line species given in Table VIII have large errors reflecting the very poor quality of the spectra. In discussing the fits to the spectra it should be noted that in a quadrupole split spectrum the relative line positions are given as a function of e^2qQ and δ by equation III-7

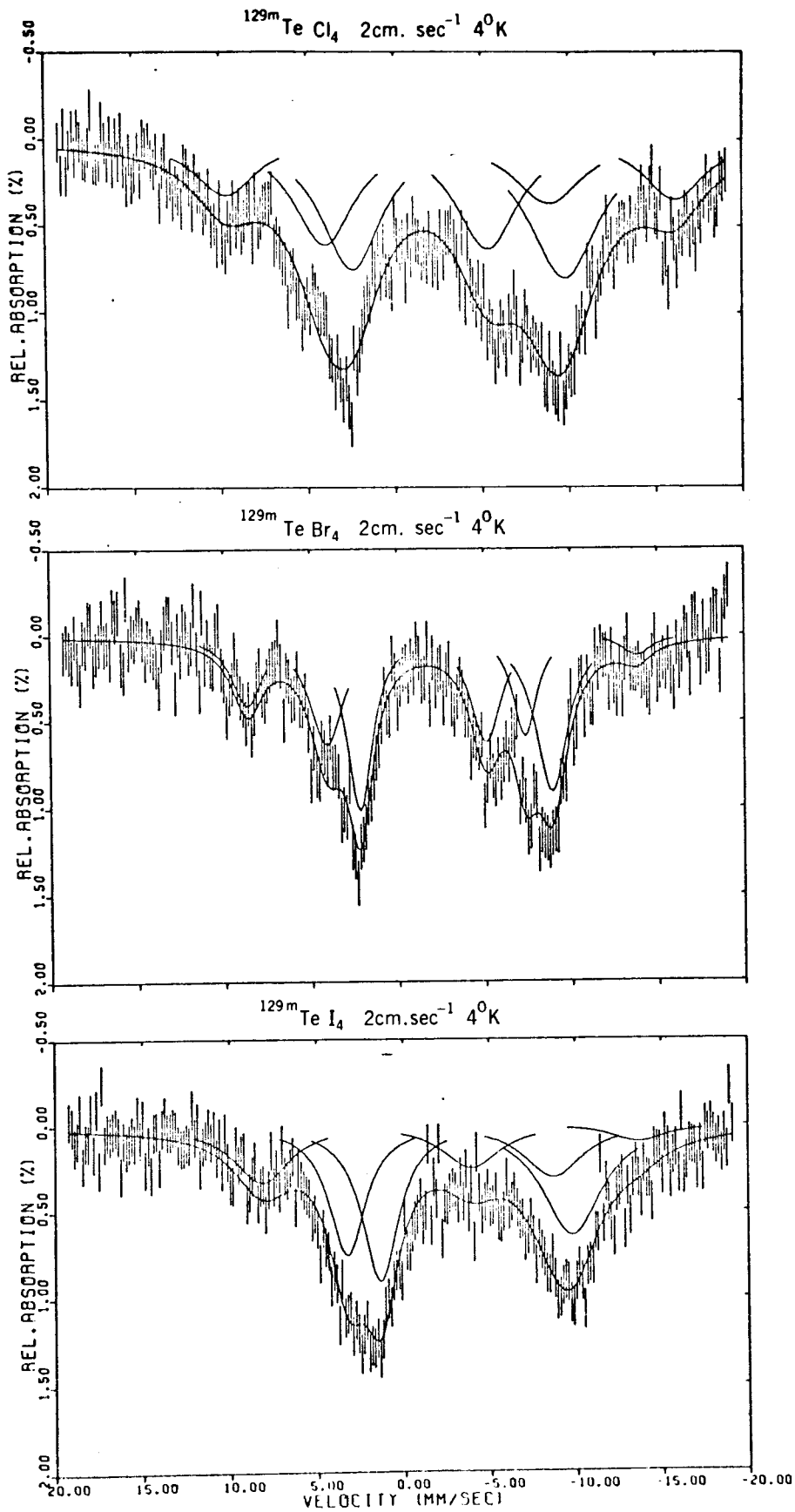


Figure 14. ^{129}I Emission Spectra of the TeX_4
(X = Cl, Br, I) Compounds.

TABLE VIII

A. $\text{Te}^{129}\text{I}_4$ Mössbauer Emission Parameters.

Compound	Species I		Species II		$\frac{\chi^2}{N}$
	$^{129}\delta_a$	e^2qQ_a	$^{129}\delta_a$	e^2qQ_a	
Temp. °K	mm. sec. $^{-1}$	Mc. sec. $^{-1}$	mm. sec. $^{-1}$	Mc. sec. $^{-1}$	% Intensity
$^{129\text{m}}\text{TeCl}_4$	3.5 ± 0.7	-2100 ± 200	$0.2 \pm .2$	5.2 ± 0.8	22
$^{129}\text{TeCl}_4$	2.8 ± 0.3	-2000 ± 100	$0.2 \pm .1$	5.0 ± 0.2	35
$^{129\text{m}}\text{TeBr}_4$	3.0 ± 0.4	-1900 ± 100	$0.2 \pm .2$	4.4 ± 0.2	16
$^{129\text{m}}\text{TeI}_4$	2.9 ± 0.4	-1400 ± 150	$0.2 \pm .2$	2.7 ± 0.7	9

B. $\text{Te}^{129}\text{I}_4$ Mössbauer Absorption Parameters.

Temp. °K	$^{129}\delta_a$		η	%	$\frac{\chi^2}{N}$
	mm. sec. $^{-1}$	Mc. sec. $^{-1}$			
Species I	1.1 ± 0.3	-1200 ± 200	0.28 ± 0.17	66.7	1.44
Species II	0.35 ± 0.2	320		33.3	

a. δ and e^2qQ are relative to a ZnFe source in an absorption experiment.

b. Intensity expressed as a % of the total resonance absorption observed.

and that the relative line intensities must be in accord with the square of the Clebsh-Gordon coefficients (Fig.4) for the various transitions. Thus if a statistically acceptable computer fit can be obtained which gives line positions in accord with equation III-7 and relative intensities in reasonable agreement with the theoretical values, then the fit may be judged to be a good one.

The line widths observed in the spectra were again very broad.

3. The Emission Spectrum of $^{129}\text{TeCl}_4$.

The rearrangement or molecular decomposition which appears to accompany the decay in the $^{129\text{m}}\text{TeCl}_4$ compounds may have originated in the extensive electronic excitation accompanying the $^{129\text{m}}\text{Te} \rightarrow ^{129}\text{Te}$ isomeric transition. In this case it was found possible to check this possibility by rapidly preparing TeCl_4 labelled with ^{129}Te and measuring the emission spectrum at 4°K before the 69 min. source had decayed away. A comparison of typical spectra for $^{129\text{m}}\text{TeCl}_4$ and $^{129}\text{TeCl}_4$ is shown in Figure 15. It can be seen that the two spectra were very similar in their general features, although the single line component in the $^{129}\text{TeCl}_4$ source appeared to be more prominent than that in the $^{129\text{m}}\text{TeCl}_4$ source.

It should be noticed that the % absorption for the $^{129}\text{TeCl}_4$ source is much larger (ca. 4.5%) than

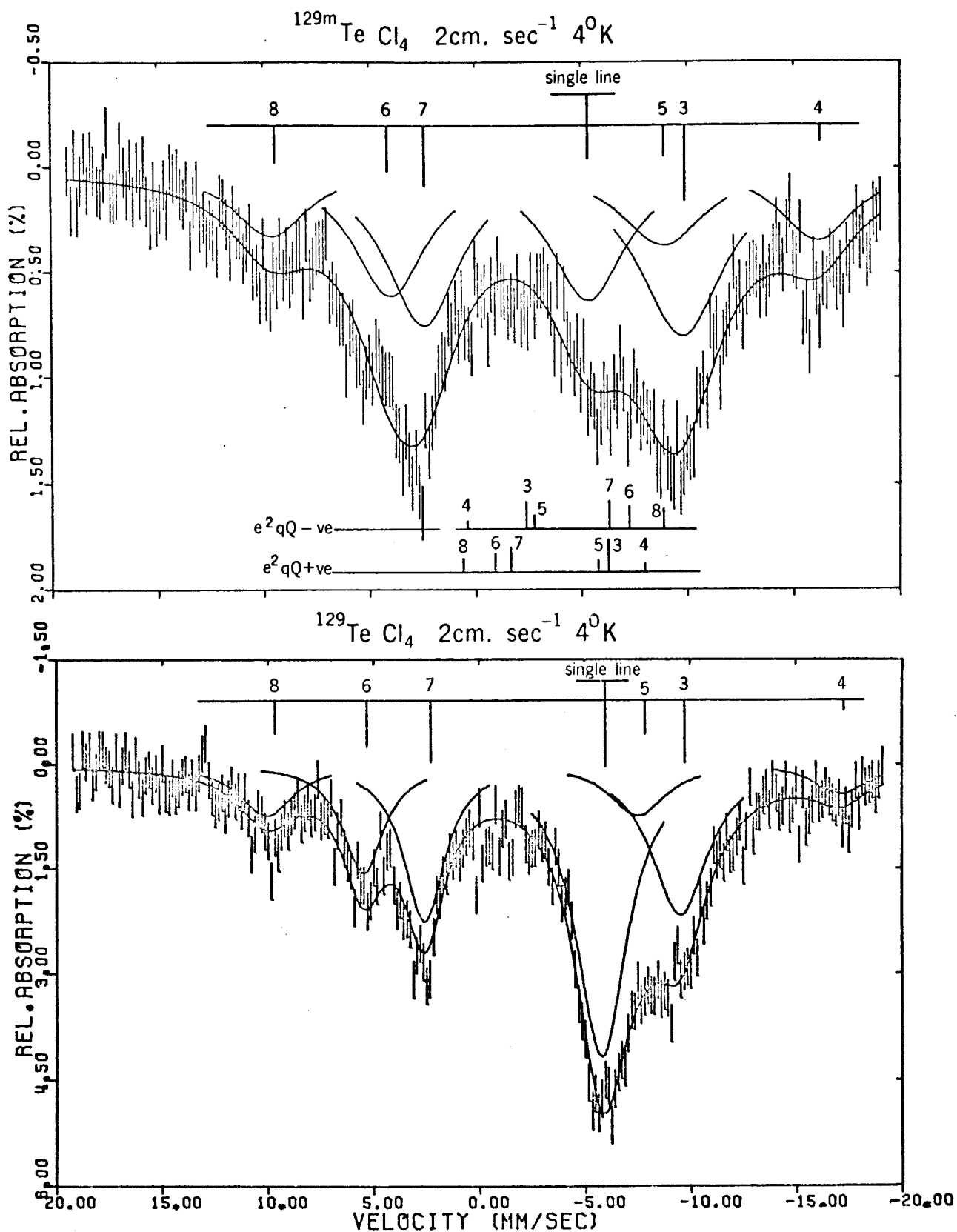


Figure 15. ^{129}I Emission Spectrum of TeCl_4 .

that for the $^{129m}\text{TeCl}_4$ source (ca. 1.5%) because in the former there is no tellurium γ -ray background arising from the $^{129m}\text{Te} \longrightarrow ^{129}\text{Te}$ isomeric transition. The larger % effect and the apparently narrower linewidths for the ^{129}Te source lead to a much more clearly resolved spectrum and the individual components in the spectrum are more obvious in this case. The increased relative intensity of the single-line component in the spectrum in essence provides supporting evidence that such a component does exist, it being much less obvious in the case of $^{129m}\text{TeCl}_4$.

4. The Absorption Spectrum of $\text{Te}^{129}\text{I}_4$.

The Mössbauer absorption experiment with a $\text{Zn}^{129m}\text{Te}$ source versus a ^{129}I labelled TeI_4 absorber, was performed in order to observe the Te-I bond from the point of view of the ligand. Two quadrupole split species were observed, one with a very large quadrupole splitting and small isomer shift and the other with a small quadrupole coupling and large isomer shift. (Unfortunately the parameters obtained (Table VIII B) could not be related to the emission Mössbauer data.)

XI Discussion of the ^{125}Te Mössbauer Absorption Spectra.

A. Significance of TeX_6^{2-} Isomer Shifts.

For the compounds $(\text{NH}_4)_2\text{TeX}_6$, $\text{X} = \text{Cl}, \text{Br}$ or I , it is apparent that the Mössbauer isomer shifts increase in the series $\delta(\text{TeI}_6^{2-}) < \delta(\text{TeBr}_6^{2-}) < \delta(\text{TeCl}_6^{2-})$ (Table VI). As pointed out in the introduction Rex-Rgnd is positive for the ^{125}Te Mössbauer transition indicating that the increase in isomer shift in the TeX_6^{2-} series corresponds to an increase in s-electron density on tellurium. If there are two electrons localised in the 5s orbital, the tellurium nucleus becomes deshielded as p-electrons are removed in bonding to the ligand halogens. The increasing electronegativity of the halogens, where $\text{I} < \text{Br} < \text{Cl}$, results in greater removal of p-electrons from the tellurium which in turn causes an increase in the s-electron density on tellurium.

Previously reported N.Q.R. data along with the Mössbauer information reported here, allows the above theory to be represented more quantitatively. It can be shown that a linear relationship exists between the number of holes h_p in the 5p shell on the tellurium atom as calculated from N.Q.R., and the ^{125}Te Mössbauer isomer shifts for the TeX_6^{2-} anions. Nakamura et al.^[41] have measured the halogen N.Q.R. spectra of these octahedral ions and utilizing the theory of Townes and Dailey^[27], calculated the net charge, ρ , on the tellurium atom. For octahedral ions

$$\rho = 4 - 6(1 - i)$$

(XI-1)

where i is the ionicity of the bond. In determining $(1 - i)$ it was assumed that the ligand halogen employs 15% s-character in bonding to the tellurium. This simplifying assumption may not be completely valid^[98], however in the absence of any other approach to this problem we have assumed Nakamura's estimates of the net charge on the tellurium to be accurate values. If one assumes that only tellurium 5p electrons are involved in bonding, the values for hp on tellurium can be directly obtained from the N.Q.R. ρ values (Table IX). The isomer shift for CaTe recorded by Jung and Triftshäuser is also included in Table IX and it is assumed that in CaTe , the tellurium is present as the Te^{2-} ion, i.e. $hp = 0$.

Table IX

The Tellurium 5p Shell Electron Populations and the ^{125}Te Mössbauer Isomer Shifts of the TeX_6^{2-} Ions (X = Cl, Br, I)

Compound	ρ	hp	δ mm. sec. ⁻¹ ^a
$(\text{NH}_4)_2\text{TeCl}_6$	+2.08	4.08	1.70 \pm 0.10
$(\text{NH}_4)_2\text{TeBr}_6$	+1.48	3.48	1.40 \pm 0.1.
$(\text{NH}_4)_2\text{TeI}_6$	+0.88	2.88	1.09 \pm 0.13
Te^{2-}	-2.00	0.00	-0.14 \pm 0.07 ^b

a with respect to a $\text{Cu}/^{125}\text{I}$ source.
 b Jung and Triftshäuser^[11].

A plot of this data gives the linear solution:

$$\delta(\text{mm. sec.}^{-1}) = (0.45 \pm 0.01)hp - (0.15 \pm 0.03) \\ (\text{I/Cu sources}) \quad (\text{XI-2})$$

The above expression is considerably different from that predicted by Ruby and Shenoy^[39] who calculated $|\psi_s(0)|^2$ values for various electronic configurations of tellurium and then related them to the Mössbauer isomer shifts for a number of tellurium compounds. These workers concluded that δ should shift by 0.3 mm. sec.⁻¹ for each 5p hole. However, their work may be criticised since the electronic configurations that they assigned to various tellurium compounds would appear to be unreasonable. For example, they proposed that in TeI_6^{2-} , the tellurium has the configuration $5s^2 5p^0$, which is a totally unreasonable assumption.

B. Significance of the TeX_4 Isomer Shifts and Quadrupole Couplings.

1. Isomer Shift .

The tellurium tetrahalides TeX_4 , where $X = \text{Cl}$, Br and I , all have identical isomer shifts. This suggests a similar removal of 5p electrons from the tellurium in TeCl_4 , TeBr_4 and TeI_4 . The change in electronegativity

of halogen appears to be offset by a rearrangement in the geometry about the central tellurium atom. Thus whereas in TeCl_4 , there are three short covalent Te - Cl bonds and three long Te --- Cl bridging bonds [60], in TeI_4 the environment about the tellurium may in fact be much closer to octahedral with six long Te - I bonds. Then an increased effective co-ordination around tellurium with a corresponding increase in the removal of p-electrons would counteract the decrease in ligand electronegativity.

2. Quadrupole Coupling e^2qQ

The small e^2qQ values observed for the TeX_4 compounds are consistent with a pseudo-octahedral environment around the tellurium. The quadrupole coupling decreases with $\text{TeCl}_4 > \text{TeBr}_4 > \text{TeI}_4$ as the electronegativity of the ligand decreases, this being consistent with the above discussion.

XII Discussion of the ^{129}I Mössbauer Spectra.

A. Identification of the IX_6^- Anions.

There are three pieces of evidence that identify the IX_6^- ions in the Mössbauer emission spectra of the $^{129\text{m}}\text{TeX}_6^{2-}$ compounds:

1. For isostructural and isoelectronic species, a constant isomer shift ratio $\delta(^{125}\text{Te})/\delta(^{129}\text{I})$ is observed. A plot of the ^{125}Te isomer shifts for isoelectronic and isostructural molecules including the compounds studied here gives a straight line of slope:

$$\frac{\delta(^{125}\text{Te})}{\delta(^{129}\text{I})} = 0.29 \pm 0.01 \quad (\text{XII-1})$$

(Figure 16). The linearity of this plot is supporting evidence for the formation of the IX_6^- anions in radioactive decay.

Similar isomer shift plots have been reported by Jung and Triftshäuser^[11] for $^{125}\text{Te} - ^{127}\text{I}$, by Ruby and Shenoy^[39] for $^{125}\text{Te} - ^{129}\text{I}$, $^{121}\text{Sb} - ^{125}\text{Te}$ and $^{127}\text{I} - ^{129}\text{Xe}$ and by Jones and Warren^[34] for the same $^{125}\text{Te} - ^{129}\text{I}$ plot. The graphs made by Jung and Triftshäuser and by Ruby and Shenoy were not made for isoelectronic and isostructural compounds in all cases, so as a result the linear relationships they obtained may in part have been fortuitous. The isomer shift

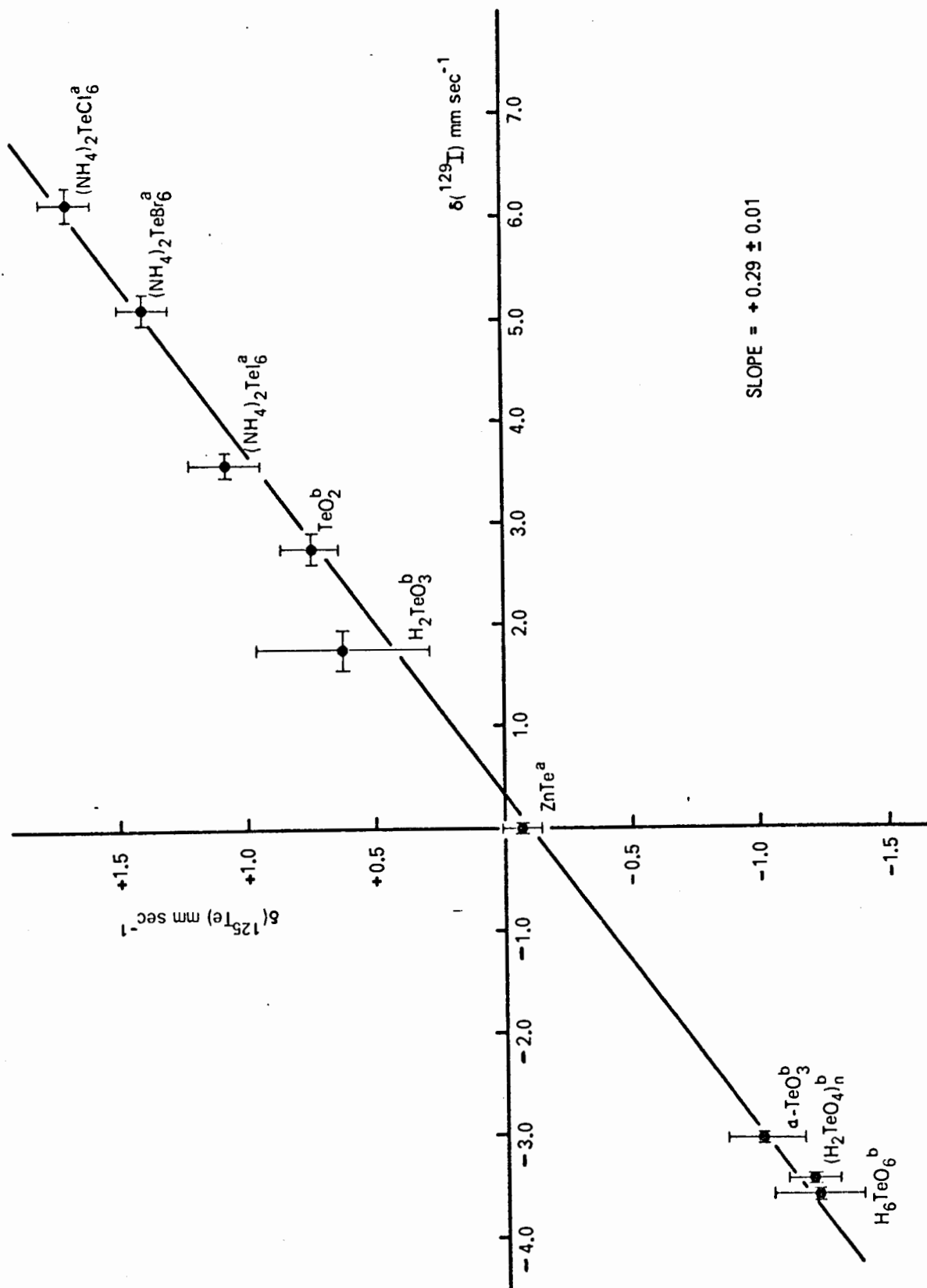


Figure 16. Isomer Shift Plot of $\delta(^{125}\text{Te})$ Versus $\delta(^{129}\text{I})$ for Isoelectronic and Isostructural Compounds.

ratio reported here is in agreement with the value of 0.29 reported by Jones and Warren^[34].

2. The isomer shift of the proposed ICl_6^- ion is consistent with that to be expected on the basis of the Mössbauer spectra of $^{127}\text{ICl}_2^-$ and $^{127}\text{ICl}_4^-$ recorded by Perlow and Perlow^[4].

The Mössbauer isomer shift recorded here for $^{129}\text{IX}_6^-$ can be related to the number of holes hp in the ^{129}I 5p shell via the equation^[26]

$$\delta(\text{mm. sec.}^{-1}) = 1.5\text{hp} - 0.54 \quad (\text{ZnTe Sources}) \quad (\text{XII-2})$$

See Table X for these data. From hp the net charge on the ^{129}I atom and the charge on the ligand can be calculated.

In the case of $^{129\text{m}}\text{TeCl}_6^{2-} \xrightarrow{\beta^-} ^{129}\text{ICl}_6^-$, the net charge on the iodine is +3.5 which corresponds to the transfer of 0.75 electrons from the I^- configuration to the chlorine ligand for each of the six I - Cl bonds and compares well with the values of 0.80 e^- and 0.75 e^- calculated recently by Ruby and Shenoy^[39]. The above analysis therefore shows that the bonding in the postulated ICl_6^- ion is consistent with the previously proposed nature of the bonding in the known stable iodine chlorine compounds. It also demonstrates that the linear relationship between hp and ^{129}I isomer shifts holds out to a value of hp = 4.5.

Table X
Comparison of Mössbauer and N.Q.R. Results.

Compound	Electronegativity Difference	$X_x - X_{Te}$	$X_x - X_I$	<u>P-holes (hp) and Charges(p).</u>				$\rho(I)$	$\rho(x)$
				N.Q.R. (15% s on X)	N.Q.R. (no s on X)	Mössbauer (^{129}I)			
$(NH_4)_2TeCl_6$	0.9	0.5	4.08	2.08	4.34	2.34	4.5 ± 0.1	3.5	-0.75
$(NH_4)_2TeBr_6$	0.7	0.3	3.48	1.48	3.93	1.93	3.7 ± 0.1	2.7	-0.62
$(NH_4)_2TeI_6$	0.45	0.0	2.88	0.88	3.34	1.34	2.7 ± 0.1	1.7	-0.45

3. In the emission spectra of the $^{129}\text{IX}_6^-$ anions a single line was observed indicating a zero e^2qQ value (Table VII). The most probable iodine species having a zero e^2qQ value and such a large isomer shift is the daughter IX_6^- anion which is isostructural and isoelectronic with the parent TeX_6^{2-} ion. The only possible alternative might be a tetrahedral IX_4 species but it is quite unrealistic to propose rearrangement to a tetrahedral geometry in this crystal environment. Moreover the isomer shift for such a molecule would probably be smaller than that observed.

B. Significance of Observing IX_6^- anions.

The IX_6^- anions where X = Cl, Br, I have not been previously prepared and the present work demonstrates that the Mössbauer effect may be used to study these ions formed in the radioactive decay $^{129\text{m}}\text{TeX}_6^{2-} \xrightarrow{\beta^-} ^{129}\text{IX}_6^-$ (X = Cl, Br, I). It must be emphasized that in the Mössbauer investigations, the daughter ions are only observed over the lifetime of the Mössbauer level (16.8 n sec.). These ions may be chemically unstable over longer times. The broadened linewidths of $2\Gamma = 1.5$ to $2.3 \text{ mm. sec.}^{-1}$ in the emission spectra when compared with the linewidths of 1.0 to $1.4 \text{ mm. sec.}^{-1}$ observed in ^{129}I absorption experiments indicate evidence of a change in the chemical environment of the ^{129}I atoms over the lifetime of the Mössbauer transition [97]. The spectra at 4°K also indicate the presence of some ^{129}I

atoms in a chemical environment other than that of the IX_6^- ion, i.e. more than one line was observed, this being most pronounced in the case of the $(\text{NH}_4)_2\text{TeI}_6$ compound. The chemical stability was observed to decrease with $\text{ICl}_6^- > \text{IBr}_6^- > \text{II}_6^-$. This may reflect the stability of the TeX_6^{2-} anions in the lattice environment.

The additional species observed in the $(\text{NH}_4)_2\text{TeX}_6$ lattices (Figure 12) may have originated from the decomposition of $^{129\text{m}}\text{TeX}_6^{2-}$ in the isomeric transition $^{129\text{m}}\text{Te} \rightarrow ^{129}\text{Te}$ rather than as a result of the chemical instability of the IX_6^- ions. The isomeric transition is highly internally converted which may lead to Auger charging and hence to an extensive molecular decomposition. For example, decomposition occurs in $\text{H}_6^{129\text{m}}\text{TeO}_6 \xrightarrow{\beta^-} \text{H}_6^{129}\text{IO}_6$, whereas in the case of $\text{H}_6^{129}\text{TeO}_6 \xrightarrow{\beta^-} \text{H}_6^{129}\text{IO}_6$, no decomposition was observed. A Mössbauer emission experiment with an $(\text{NH}_4)_2^{129}\text{TeX}_6$ source compound would have clarified this point. However, the short half-life of ^{129}Te (69 min.), and the time involved in the chemical preparation and in cooling the sample and the dewar to 4°K precluded these measurements. A probable decomposition product is the square planar IX_4^- ion. Evidence supporting this proposal is discussed later (section XII-F).

In conclusion, there is evidence that the octahedral ICl_6^- , IBr_6^- and II_6^- ions produced by radioactive decay exist over the lifetime of the Mössbauer transition. It

is interesting to note that I_7^- ions previously prepared were not octahedral but consisted of a three-dimensional array of I_3^- ions and I_2 molecules^[69].

C. Electron Recall Following β^- -Decay.

Perlow and Perlow^[6] have studied the effects of the $^{129}I \xrightarrow{\beta^-} ^{129}Xe$ radioactive decay in compounds containing the $^{129}ICl_2^-$ and $^{129}ICl_4^-$ ions. It was observed that the $XeCl_2$ and $XeCl_4$ compounds formed were stable over the lifetime of the Mössbauer transition. They calculated the charge on the iodine atom and on the daughter Xenon following the decay and observed that the increased electronegativity of the daughter xenon atom resulted in an increased electron withdrawal from the chlorine ligand. The net charge on the iodine before decay was +0.39 and following the decay, xenon had a net charge of +1.00 rather than +1.39, i.e. 0.39 electrons had been recalled from the ligands by xenon.

A similar analysis can be carried out for the results of the present work. As discussed in a preceding section, the halogen N.Q.R. data of Nakamura et al. for the TeX_6^{2-} ions allows the calculation of the charge on the central tellurium. The charge on the daughter iodine following the radioactive decay can be calculated from the Mössbauer isomer shift data using equation XII-2. The charges on the tellurium and iodine calculated from Mössbauer data are compared to those calculated from N.Q.R. data in Table X.

It is apparent that there is a discrepancy since the charge on the daughter iodine is more than +1 greater than the charge on the tellurium and this would not be expected as a result of the increased electronegativity of the atom following the decay.

A possible reason may be Nakamura's assumption of 15% s-character in the ligand halogens bonding orbital. From the equation

$$e^2q_{\text{mol}} = (1 - i)(1 - s) e^2q_{\text{atom}} \quad (\text{VII-3})$$

it can be seen that this assumption effectively reduces the charge on the central tellurium and thus its number of p-holes h_p . If this assumption is omitted from the calculation, a higher charge is obtained for the tellurium (Table X). Even then there is no measureable recall in the $\text{TeCl}_6^{2-} \rightarrow \text{ICl}_6^-$ transition while in the case of TeBr_6^{2-} and TeI_6^{2-} there is recall of 0.23 and 0.36 electrons in each case. The electronegativity differences shown in Table Y also reflect the change in the charge of the central atom.

D. ^{125}Te Isomer Shift Relationships.

A graph of the ^{125}Te Mössbauer isomer shifts for the tellurium hexahalides versus the h_p values obtained from N.Q.R. (Tables X) gives the linear solutions

(a) assuming 15% s-character

$$\delta(\text{mm. sec.}^{-1}) = (0.45 \pm 0.01)\text{hp} - (0.15 \pm 0.03)$$

(I/Cu sources) (XII-4)

and (b) assuming no s-character

$$\delta(\text{mm. sec.}^{-1}) = (0.41 \pm 0.03)\text{hp} - (0.16 \pm 0.10)$$

(I/Cu sources) (XII-5)

(Figure 17). One can use the above equations to calculate hp values on tellurium from ^{125}Te isomer shifts for other compounds assuming pure p bonding. Calculations on the tellurium tetrahalides studied in this work are discussed in a following section.

It is also interesting to note that one can convert Bukshpan's expression ^[26] for ^{129}I

$$\delta(\text{mm. sec.}^{-1}) = 1.50 \text{ hp} - 0.54 \text{ (ZnTe sources)}$$

by multiplying by the isomer shift ratio

$$\frac{\delta(^{125}\text{Te})}{\delta(^{129}\text{I})} = 0.29 \pm 0.01$$

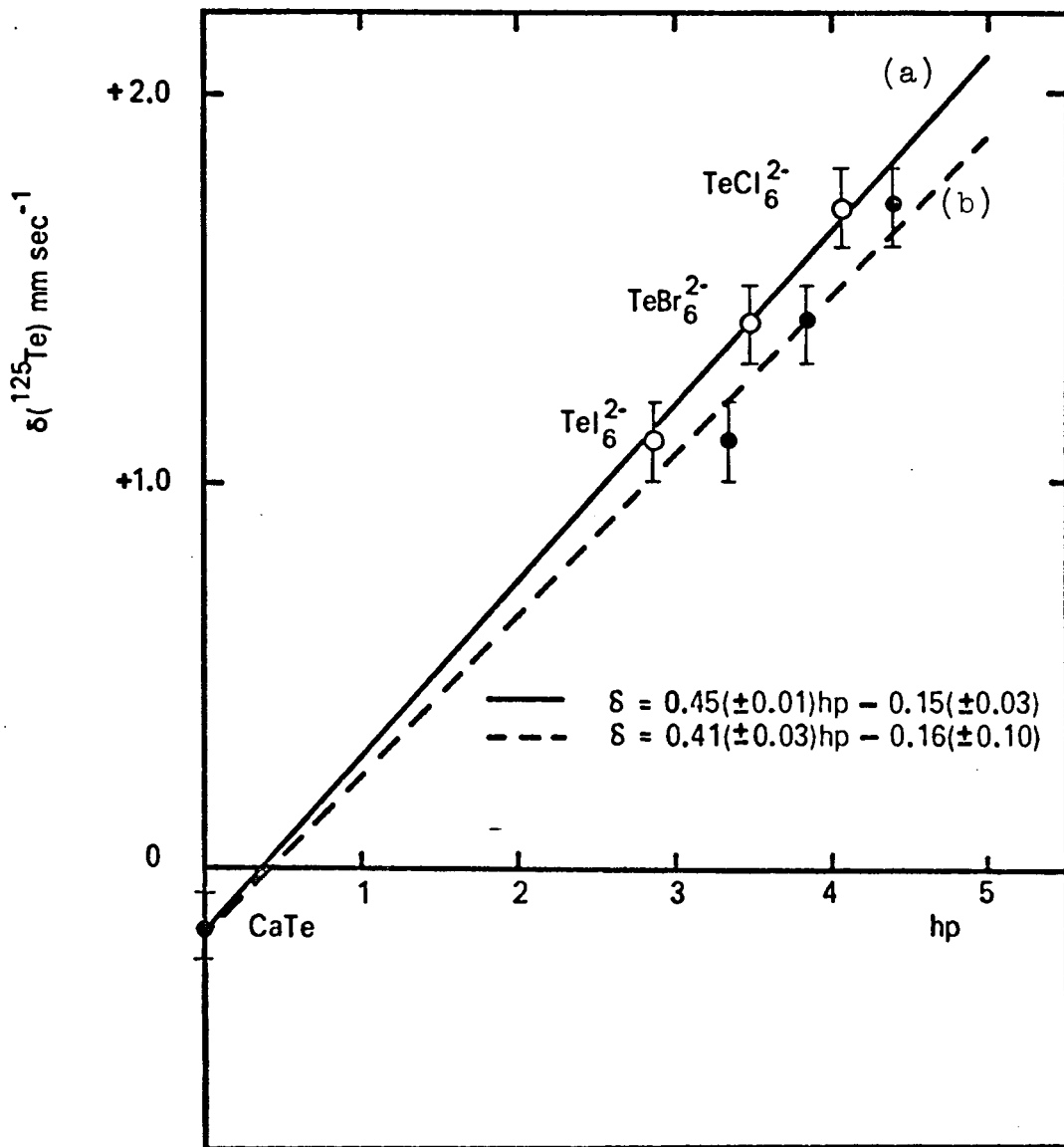


Figure 17. Comparison of $\delta(^{125}\text{Te})$ Versus hp From N.Q.R. Data Assuming (a) 15% and (b) No s -Character in the Halogen Bonding Orbitals.

which then gives for ^{125}Te isomer shifts

$$\delta(\text{mm. sec.}^{-1}) = 0.44 \text{ hp} - 0.16 \text{ (ZnTe sources)}$$

$$\text{or } \delta(\text{mm. sec.}^{-1}) = 0.44 \text{ hp} - 0.23 \text{ (I/Cu sources)} \quad (\text{XII-6})$$

This expression agrees within experimental error with the relationships obtained in this work, directly from the ^{125}Te Mössbauer data (equations XII-4 and XII-5). This lends some support to the interpretation of the tellurium hexahalide data which lead to equations (XII-4) and (XII-5).

To determine unequivocally whether or not the ligand halogen in TeX_6^{2-} employs any s-character in bonding it will be necessary to measure this parameter in a more direct way. For example the ^{129}I Mössbauer absorption spectrum of $(\text{NH}_4)_2\text{Te}^{129}\text{I}_6$ would provide some evidence for or against s-participation.

E. Possibility of d-Orbital Participation in Bonding.

It is of interest to compare the above analysis with the theoretical discussions in the literature which incorporate d-orbitals in the bonding scheme.

Semi-empirical L.C.A.O.-M.O. calculations have recently been carried out on the TeCl_6^{2-} ion^[42] and computational verification of the "inert pair effect" of the tellurium $5s^2$ electrons was achieved. Self consistent

charges and orbital occupations in TeCl_6^{2-} were calculated, and from these the ^{35}Cl nuclear quadrupole coupling constant for the molecular ion was calculated to be -26.90 MHz., which compares well with the experimental one of 29.99 MHz.

These workers also calculated a charge of $+1.03$ on the central tellurium atom. This is lower than the value of $+2.08$ calculated by Nakamura et al. using the Townes and Dailey theory because of the incorporation of d-orbitals in the bonding scheme.

Also the s-character of the chlorine sigma bond in TeCl_6^{2-} was calculated to be 0.1 , as compared to 0.15 assumed in the calculations done by Nakamura et al..

Other workers^[48, 49] have also suggested involvement of d-orbitals in the bonding of the ions ICl_2^- and ICl_4^- . They suggested that the iodine d-orbitals are probably strongly polarized toward the chlorine atoms. However the principal sources of bonding were assumed to be molecular orbitals consisting of iodine p-orbitals. These calculations also revealed that when the number of ligands is high, thus increasing the formal positive charge on the central atom, excited molecular orbitals must be involved in bonding (i.e. d-orbital participation). This may be the case with the TeX_6^{2-} and IX_6^{2-} ions studied here, which have a higher number of ligands than ICl_2^- and ICl_4^- .

However, the calculated charge of $+1.3$ on tellurium in TeCl_6^{2-} is too small to be consistent with the charge calculated from the Mössbauer experiments on the central iodine

after β -decay. Therefore, no definite conclusion can be made on d-orbital participation in the bonding scheme of iodine or tellurium in these compounds [27, 36].

Another possible bonding scheme involves the "inert" tellurium 5s electron pair in bonding. It has been shown from electronic spectra [99] that the 5s electrons exist in the $a_{1g}\sigma^*$ level in the TeCl_6^{2-} and TeBr_6^{2-} and that a small amount of participation of the $a_{1g}\sigma^*$ electrons in bonding occurs. However as discussed above a consistent interpretation of the Mössbauer and N.Q.R. data can be made without the use of s- or d-orbitals in the bonding scheme.

F. The Decay Products of $^{129m}\text{TeX}_4$.

The daughter molecules resulting from the β -decay of the $^{129m}\text{TeX}_4$ were not isostructural and isoelectronic with the parent molecules. This conclusion was reached by comparing the experimentally observed ^{129}I isomer shifts and quadrupole couplings with the values calculated for the isoelectronic species from ^{125}Te absorption using the relationships $\delta(^{125}\text{Te})/\delta(^{129}\text{I}) = 0.29 \pm 0.01$ and $\frac{e^2qQ(^{125}\text{Te})}{e^2qQ(^{129}\text{I})} (1 + \frac{\eta^2}{3})^{\frac{1}{2}} = 0.45$ (Table XI). The sign of e^2qQ cannot be determined from ^{125}Te absorption experiments, therefore two possible sets of line positions may occur as shown in Table XII and Figure 15 for TeCl_4 .

It is immediately apparent that the observed and predicted line positions do not coincide. Thus with

Table XI

Predicted ^{129}I δ and e^2qQ from ^{125}Te Data.

	Experimental ^{125}Te δ (mm. sec. $^{-1}$) (Mc. sec. $^{-1}$)	Predicted ^{129}I δ (mm. sec. $^{-1}$) (Mc. sec. $^{-1}$)	Experimental ^{129}I δ (mm. sec. $^{-1}$) (Mc. sec. $^{-1}$)	Experimental ^{129}I e^2qQ (Mc. sec. $^{-1}$)
TeCl_4	1.0	3.8	3.5	2105
TeBr_4	1.1	4.1	3.0	1852
TeI_4	1.0	3.8	2.9	1394

Table XII

A Comparison of the Predicted Line
Positions for $^{129}\text{ICl}_4^+$ Mössbauer Emission with
the Experimentally Observed Positions

LINE	Predicted* (mm. sec. ⁻¹)		Experimental (mm. sec. ⁻¹)
	e ² qQ(-)	e ² qQ(+)	
1	10.3	-18.0	
2	5.4	-13.1	
3	-1.9	- 5.8	- 9.4
4	.1	- 7.9	-15.6
5	-2.3	- 5.4	- 8.5
6	-7.2	- 0.5	4.1
7	-6.2	- 1.6	2.5
8	-8.6	.9	9.6

* For method of prediction see page 81.

$^{129m}\text{TeCl}_4$ and $^{129}\text{TeCl}_4$, the ^{129}I formed in the radioactive decay was not found in an environment isoelectronic and isostructural with that of the tellurium in the parent. Therefore, rearrangement must have accompanied the decay in a large fraction of events. A similar observation was made for the $^{129m}\text{TeBr}_4$ and $^{129m}\text{TeI}_4$ sources.

The question arises as to the identity of the iodine species formed in the TeX_4 lattices. The computed parameters for the $^{129m}\text{TeCl}_4$, $^{129m}\text{TeBr}_4$ and $^{129m}\text{TeI}_4$ sources are shown in Table VIII. The very large errors reflect the poor quality of the spectra. The Mössbauer parameters η , e^2qQ and δ have allowed calculations of orbital populations U_i and the charge on the iodine species using equations V-3 and V-9 discussed in the introduction (Table XIII). The orbital populations U_x , U_y , and U_z indicate a square planar configuration for the iodine tetrahalide β -decay products. For a square planar ion with two non-bonding electrons in the out of plane orbital, $U_z = 2$, $U_x = U_y$ and $2U_p = -h_p$. The orbital populations calculated for the tetrahalides (Table VIII) appear to agree well with these relations. A comparison of the ^{127}I Mössbauer absorption parameters for the square planar $\text{ICl}_4^{-[4]}$ ion with the emission parameters recorded here for the decay of $^{129m}\text{TeCl}_4$ (converted to ^{127}I parameters via equations VI-1 and VI-2) is also shown in Table XIII.

Table VIII

A. Table of Orbital Populations U_i and h_p
Values for the ^{129m}Te Mössbauer Emission
Data in the Decay ^{129m}TeX₄ $\xrightarrow{\beta^-}$ ¹²⁹I_X₄⁺.

	h _p	U _p	U _x	U _y	U _z	Charge on Central I
^{129m} TeCl ₄	2.7 ± 0.5	-1.3 ± 0.1	0.6	0.7	2.0	+1.7
^{129m} TeBr ₄	2.4 ± 0.3	-1.2 ± 0.1	0.75	0.9	2.0	+1.4
^{129m} TeI ₄	2.3 ± 0.3	-0.9 ± 0.1	1.0	1.0	1.8	+1.3

B. Comparison of ^{129m}TeCl₄ Emission and
¹²⁷ICl₄⁻ Absorption Mössbauer Spectra.

	$e^2qQ(^{127}\text{I})$ Mc. sec. ⁻¹	$\delta(^{127}\text{I})_1$ mm. sec. ⁻¹	ref.
^{129m} TeCl ₄	+3000 ± 300	-1.3 ± 0.1	*
¹²⁷ ICl ₄ ⁻	+3094 ± 20	-1.39 ± 0.05	4

* This work.

It can be seen that the isomer shifts and quadrupole couplings for the two cases are almost identical. Consequently the decay fragments observed may be tentatively identified as square planar IX_4^- ions. This is not surprising since the ICl_4^- ion is very stable chemically. The identification of the single lines observed in the spectra is far from clear, but its isomer shift is similar to that expected for an IX_6^- ion. The possibility of it being the I^- ion is ruled out because the isomer shift is much too large. In Figure 15, one can see that the intensity of the single line increased when a $^{129}\text{TeCl}_4$ source was used, thus bypassing the $^{129\text{m}}\text{Te} - ^{129}\text{Te}$ isomeric transition. If the single line was caused by the presence of octahedral IX_6^- ions in the crystal, this implies that the formation of the IX_6^- ion is preferred when there is less disruption in the crystal due to nuclear decay. In contrast, the formation of the IX_4^- ion appears to be preferred when there is more electronic excitation in the crystal, as was the case when a $^{129\text{m}}\text{TeCl}_4$ source was used. This is consistent with the pseudo-octahedral environment around the tellurium atom in the source compound TeX_4 (Fig. 8). This environment should be retained when there is less electronic excitation in the crystal.

One can conclude that the isomeric transition $^{129m}\text{Te} \rightarrow ^{129}\text{Te}$ was not the sole factor resulting in the rearrangement of the tetrahalide molecules. The cause of the rearrangement has not been established and would be a good point for further study.

XIII Conclusion.

The ^{129}I Mössbauer emission spectra of the $(\text{NH}_4)_2\text{TeX}_6$ compounds have provided firm evidence for the formation of the octahedral IX_6^- ions in the crystal as a result of the radioactive decay $^{129\text{m}}\text{Te} - ^{129}\text{I}$. The ^{129}I isomer shifts for these ions are in good agreement with those values predicted from the ^{125}Te isomer shifts of the parent compounds using the isomer shift ratio $\delta(^{125}\text{Te})/\delta(^{129}\text{I}) = 0.29$ (Table XI). This ratio was arrived at from Mössbauer measurements on isoelectronic and iso-structural tellurium and iodine compounds (Figure 16).

As in all Mössbauer emission experiments, the presence of the daughter ions is only observed over the lifetime of the Mössbauer transition ($t_{1/2} = 16.8$ nsec.), and these ions may be unstable over a longer period of time. Nevertheless, the present observations are unique since a chemical synthesis of these ions has not yet been reported. The spectra at 4°K (Figure 12) also indicate the presence of ^{129}I atoms in a chemical environment other than that of the octahedral IX_6^- ions, i.e. a product giving rise to a very

large e^2qQ value was observed, this being most pronounced in the case of $(\text{NH}_4)_2\text{TeI}_6$. These products may have arisen from molecular fragmentation which can accompany the electronic excitation due to Auger charging in the $^{129\text{m}}\text{Te} - ^{129}\text{Te}$ isomeric transition, or from chemical decomposition of the daughter IX_6^- anion following the beta decay. It was not possible to distinguish between these two possibilities. A probable decomposition product is the square planar IX_4^- ion.

The daughter molecules resulting from the beta decay of the $^{129\text{m}}\text{TeX}_4$ compounds were not isostructural and isoelectronic with the parent molecules. This was concluded on comparing the experimentally observed ^{129}I isomer shifts and quadrupole couplings with the values predicted from the ^{125}Te absorption data (Table XI). Two decay fragments were observed, one exhibiting a large quadrupole coupling and the second a single line. These fragments are tentatively identified as a square planar IX_4^- ion and an octahedral IX_6^- ion. The firmest evidence for the proposed formation of the IX_4^- ion was found in the case of TeCl_4 , where the ^{127}I Mössbauer

absorption parameters previously recorded for the square planar $^{127}\text{ICl}_4^-$ ion were found to be consistent with the ^{129}I emission parameters recorded in this work (Table XIII). The iodine 5p orbital populations arrived at from the isomer shifts and quadrupole splittings of the emission spectra also indicate a square planar configuration for the iodine tetrahalide beta decay products. The identification of the single line observed in the spectra is far from clear, but its isomer shift is similar to that expected for IX_6^- .

For TeCl_4 both the $^{129\text{m}}\text{Te}$ and ^{129}Te sources were studied and shown to yield essentially the same spectrum (Figure 15). Thus the extensive molecular rearrangement observed following the radioactive decay does not appear to arise from the Auger charging in the $^{129\text{m}}\text{Te} - ^{129}\text{Te}$ isomeric transition but appears to reflect the inherent relative chemical stabilities of the possible fragments which can be formed. The daughter IX_3^+ fragment would appear to be far less chemically stable than the square planar IX_4^- ion, and molecular rearrangement must occur in a time shorter than the lifetime of the Mössbauer transition.

Aside from the observation of some unusual

^{129}I -labelled polyhalide ions, the above studies have also shown that the chemical stabilities of the parent lattices and the daughter fragments appear to play a dominant role in leading to the observed products. In contrast, electronic excitation in the $^{129\text{m}}\text{Te} - ^{129}\text{Te}$ isomeric transition or in the $^{129}\text{Te} - ^{129}\text{I}$ beta decay do not appear to greatly influence the nature of the products observed.

Why rearrangement was observed in the case of the $^{129\text{m}}\text{TeX}_4$ sources and not in the case of the $(\text{NH}_4)_2^{129\text{m}}\text{TeX}_6$ sources is not clear. In the TeX_6^{2-} ions there are six long bonds, whereas in the TeX_4 compounds there is present the TeX_3^+ group (Figure 8), with three short covalent bonds. In the beta decay the oxidation state of the atom is increased by one, which results in a corresponding decrease in the atomic size. Thus steric factors may be the cause of the instability of the IX_3^+ group.

The ^{125}Te Mössbauer absorption data for the $(\text{NH}_4)_2\text{TeX}_6$ compounds have also provided information which may be useful in the general interpretation of ^{125}Te isomer shifts. Using the ^{125}Te Mössbauer isomer shifts for the TeX_6^{2-} ions and the holes, hp, in the 5p shell of the tellurium atom as calculated from

N.Q.R. data, the quantitative relationship for the isomer shift

$$\delta(\text{mm. sec.}^{-1}) = (0.45 \pm 0.01)\text{hp} - (0.15 \pm 0.03) \text{ (I/Cu sources)}$$

was found to exist. As discussed in section XII-C, there is a discrepancy between the net charge on the iodine in the hexahalides calculated from the Mössbauer emission data as compared to that on tellurium obtained from N.Q.R. data. The reason for this discrepancy may be Nakamura's assumption of 15 per cent s-character in the ligand halogen's bonding orbital. If this assumption is omitted from the calculation a closer correlation is obtained between the charges. This implies that the s-character obtained from the Townes and Dailey theory for diatomic molecules in the gaseous state, and which was used by Nakamura in his analysis, can not be extended directly to solid state systems.

However, one can conclude that the ^{129}I Mössbauer data, the $^{125}\text{Te} - ^{129}\text{I}$ isomer shift ratio obtained from Mössbauer emission and absorption data and the tellurium charges obtained from the N.Q.R. data using the Townes and Dailey approach are all reasonably consistent and support the pure p-bonding model proposed for the tellurium and iodine compounds studied in this work.

XIV. List of References.

1. A.G. Maddock, Chem. in Brit., 287 (1970).
2. S. Wexler, Actions Chimiques et Biologiques des Radiations, 8, 107 (1965).
3. S.I. Bondarevskii, A.N. Murin and P.P. Seregin
Russ. Chem. Rev., 40, 51 (1971).
4. G.J. Perlow and M.R. Perlow, J. Chem. Phys., 45, 2193(1966).
5. M. Pasternak, Symp. Faraday Soc., 1, 119 (1967).
6. Symp. Chemical Effects Associated with Nuclear Reactions and Radioactive Transformations, Vienna, December 7 - 11, 1964 (I.A.E.A., Vienna, 2 Vol., 1965) II 443.
7. J.L. Warren, The Chemical Effects of Nuclear Transformations in Some Tellurium Compounds, Ph.D. Thesis, Simon Fraser University (1971).
8. P. Rother, F. Wagner and U. Zahn, Radiochim. Acta, 11, 203 (1969).
9. M. Pasternak and T. Sonnino, Phys. Rev., 164, 384 (1967).

10. C.E. Violet and R. Booth, Phys. Rev., 144, 225 (1966).
11. P. Jung and W. Triftshäuser, Phys. Rev., 175, 512 (1968).
12. R.L. Mössbauer, Soviet Phys. Uspekshi, 3, 866 (1961).
13. H. Frauenfelder, The Mössbauer Effect, (W.A. Benjamin Inc., New York, 1962).
14. V.I. Goldanski, The Mössbauer Effect and its Applications in Chemistry, (Consultants Bureau, New York, 1964).
15. The Mössbauer Effect and its Application in Chemistry, R.F. Gould, ed. (American Chemical Society Publications, Washington, D.C. 1967).
16. G.K. Wertheim, Mössbauer Effect: Principles and Applications, (Academic Press, New York, 1964).
17. R. Bersohn, J. Chem. Phys., 20, 1505 (1952).
18. A.M. Babeshkin, E.V. Lamykin, V.A. Lebedev and A.N. Nesmeyanov, Vestn. Mosk. Univ. Khim., 11, 117, (1970).
19. K.V. Makariunas, R.A. Kalinauskas and R.I. Davidsonis, Soviet Physics JETP., 33, 848 (1971).

20. John F. Ullrich, ^{125}Te Mössbauer Effect Study of Radiation Effects and Magnetic Hyperfine Interactions in Tellurium Compounds, Ph.D. Thesis, (University Microfilms, Inc., Ann Arbor, Michigan 1967).
21. D.S. Urch, J. Chem. Soc., 5775 (1964).
22. M.H. Cohen, Phys. Rev., 96, 1278 (1954).
23. D.W. Hafemeister, R.G. DePasquali and H. DeWaard, Phys. Rev., 135, B1089 (1964).
24. S. Bukshpan, C. Goldstein, J. Sonnino and J. Shamir, J. Chem. Phys., 51, 3976 (1969).
25. M. Pasternak and T. Sonnino, J. Chem. Phys., 48, 1997 (1968).
26. S. Bukshpan, C. Goldstein and T. Sonnino, J. Chem. Phys., 49, 5477 (1968).
27. B.P. Dailey and C.H. Townes, J. Chem. Phys., 23, 118 (1955).
28. C.I. Wynter, J. Hill and W. Bledsoe, J. Chem. Phys., 50, 3872 (1969).
29. S. Bukshpan and T. Sonnino, J. Chem. Phys., 48, 4442 (1968).

30. B.S. Ehrlich and M. Kaplan, J. Chem. Phys., 50, 2041 (1969).
31. B.S. Ehrlich and M. Kaplan, Chem. Phys. Letters, 3, 161 (1969).
32. S. Bukshpan and R.H. Herber, J. Chem. Phys., 46, 3375 (1967).
33. M. Pasternak and T. Sonnino, J. Chem. Phys., 48, 2009 (1968).
34. C.H.W. Jones and J.L. Warren, J. Chem. Phys., 53, 1740 (1970).
35. K. Reddy, F. Barros and S. De Benedetti, Phys. Letters, 20, 297 (1966).
36. G.J. Perlow and M.R. Perlow, J. Chem. Phys., 48, 955 (1968).
37. D.A. Shirley, Rev. Phys. Chem., 20, 25 (1969).
38. R. Livingston and H. Zeldes, Phys. Rev., 90, 609 (1953).
39. S.L. Ruby and G.K. Shenoy, Phys. Rev., 186, 326 (1969).
40. J.L. Warren, Reference 7, p 163.

41. D. Nakamura, K. Ito and M. Kubo, J. Am. Chem. Soc., 84, 163 (1962).
42. T.B. Brill, Z.Z. Hugus Jr. and A.F. Schreiner, J. Phys. Chem, 74, 2999(1970).
43. T.L. Brown and L.G. Kent, J. Phys. Chem., 74, 3572 (1970).
44. M. Kubo and D. Nakamura, Adv. in Inorg. and Nucl. Radiochem., 48, 257 (1966).
45. D. Nakamura and M. Kubo, J. Phys. Chem., 68, 2986 (1964).
46. Von Albrecht Schmitt and Werner Zeil, Z. Naturforsch, 18a, 428 (1963).
47. S. Konda, E. Kakuichi and T. Shimizu, Bull. Chem. Soc. Japan, 42, 2050 (1969).
48. R.S. Yamasaki and C.D. Cornwell, J. Chem. Phys., 30, 1265 (1959).
49. C.D. Cornwell and R.S. Yamasaki, J. Chem. Phys., 27, 1060 (1957).
50. J.C. Evans and G.Y.S. Lo, Inorg. Chem., 6, 836 (1967).

51. G.A. Bowmaker and S. Hacobian, Aust. J. Chem., 21, 551 (1968).
52. D.E. O'Reilly and E.M. Peterson, J. Chem. Phys., 52, 6444 (1970).
53. G.L. Breneman and R.D. Willett, J. Phys. Chem., 71, 3684 (1967).
54. A. Sasane, D. Nakamura and M. Kubo, J. Phys. Chem., 71, 3249 (1967).
55. D. Nakamura, K. Ito and M. Kubo, Inorg. Chem., 2, 61 (1963).
56. S. Syoyama, K. Osaki and S. Kusanagi, Inorg. Nucl. Chem. Letters, 8, 181 (1972).
57. G.C. Pimentel, J. Chem. Phys., 19, 446 (1951).
58. A.C. Hazell, Acta Chem. Scand., 20, 165 (1966).
59. B. Buss and B. Krebs, Angewan. Chem., 9, 463 (1970).
60. B. Buss and B. Krebs, Inorg. Chem., 10, 2795 (1971).
61. A.K. Das and I.D. Brown, Can. J. Chem., 44, 939 (1966).
62. K.W. Bagnall, R.W.M. D'Eye and J.H. Freeman, J. Chem. Soc., 3385(1956).

63. Von Amador Angoso, H. Onken and H. Hahn, Z. Anorg. Allg. Chemie, 328, 223 (1964).
64. E.E. Aynsley and G. Hetherington, J. Chem. Soc., 2802 (1953).
65. C.B. Shoemaker and S.C. Abrahams, Acta Cryst., 18, 296 (1965).
66. W.R. Blackmore, S.C. Abrahams and J. Kalnajs, Acta Cryst., 2, 295 (1956).
67. S.K. Porter and R.A. Jacobson, Chem. Commun., 1244 (1967).
68. B.K. Robertson, W.G. McPherson and E.A. Meyers, J. Phys. Chem., 71, 3531 (1967).
69. E.H. Wiebenga, E.E. Havinga and K.H. Boswijk, Advan. Inorg. Chem. Radiochem., 3, 133 (1961).
70. E.H. Wiebenga and D. Kracht, Inorg. Chem., 8, 738 (1969).
71. Y. Yagi and A.I. Popov, J. Inorg. Nucl. Chem., 29, 2223 (1967).
72. Y. Yagi and A.I. Popov, Inorg. Nucl. Chem. Letters, 1, 21 (1965).

73. T. Surles, H.H. Hyman, L.A. Quarterman and A.I. Popov, Inorg. Chem., 10, 913 (1971).
74. R.A. Garrett, R.J. Gillespie and J.B. Senior, Inorg. Chem., 4, 563 (1965).
75. R.J. Gillespie, M.J. Morton, Chem. Commun., 1565 (1968).
76. R.J. Gillespie, J.B. Milne and M.J. Morton, Inorg. Chem., 7, 2221 (1968).
77. H. Stammreich and Y. Kawano, Spectrochimica Acta, 24A, 899 (1968).
78. L.Y. Nelson and G.C. Pimentel, Inorg. Chem., 7, 1695(1968).
79. R.J. Gillespie and J.B. Milne, Inorg. Chem., 5, 1577 (1966).
80. R.J. Gillespie and K.C. Malhotra, Inorg. Chem., 8, 1751 (1969).
81. K.W. Bagnall, Chemistry of Selenium, Tellurium and Polonium, (Elsevier, London, 1966) p106.
82. K.W. Bagnall, ibid., p447.

83. K.W. Bagnall, *ibid.*, p452.
84. W.A. Dutton and W.C. Cooper, Chem. Rev., 66, 657 (1966).
85. F. Feher, Handbook of Preparative Inorganic Chemistry, Vol. I, G. Brauer ed. (Academic Press, Inc., New York, 1963) p444.
86. H. Marshall, Inorganic Syntheses, Vol II, W.C. Fernellius ed. (McGraw-Hill Book Company, Inc., New York, 1946) p188.
87. J.L. Warren, Reference 7, p111.
88. L. May and D.K. Snediker, Nucl. Instr. and Methods, 55, 183 (1967).
89. G.C. Hayward and P.J. Hendra, J. Chem. Soc., A, 643, (1967).
90. I.R. Beattie and H. Chudzynska, J. Chem. Soc., A, 984 (1967).
91. P.J. Hendra and Z. Jovic, J. Chem. Soc., A, 600 (1968).
92. M.L. Unland, J. Chem. Phys., 49, 4514 (1968).

93. T.C. Gibb, R. Greatrex, N.N. Greenwood and A.C. Sarma, J. Chem. Soc., A, 212, (1970).
94. R.M. Cheyne, A ^{125}Te and ^{129}I Mössbauer Study of Complexes of Tellurium with Thiourea and Related Derivatives, Masters Thesis, Simon Fraser University (1972).
95. S.E. Gukasyan, B.Z. Iofa, A.N. Karasev, S.I. Semenov and V.S. Shpinel, Phys. Stat. Sol., 37, 91 (1970).
96. N.E. Erickson and A.G. Maddock, J. Chem. Soc., A, 1665 (1970).
97. W. Triftshäuser, Phys. Rev., 187, 491 (1969).
98. M. Kaplansky and M.A. Whitehead, Mol. Phys., 16, 481 (1969).
99. D.A. Couch, C.J. Wilkins, G.R. Rossman and H.B. Gray, J. Am. Chem. Soc., 92, 307 (1970).
100. A.J. Stone, Cambridge, England; Program described in Appendix to G.M. Bancroft, A.G. Maddock, W.K. Ong and R.H. Prince, J. Chem. Soc., A, 1967 (1966).
101. A.H. Muir Jr., K.J. Ando and H.M. Coogan, Mössbauer Effect Data Index 1958-1965, (Interscience Publishers, New York, 1966).